Entropy stable high order discontinuous Galerkin methods for nonlinear conservation laws

Jesse Chan

[1]Department of Computational and Applied Mathematics

Department of Mechanical Engineering, Rice University
August 29, 2018

High order finite element methods for hyperbolic PDEs

- Focus: high accuracy in computational mechanics on unstructured meshes.
- Applications in aerodynamics (acoustics, vorticular flows, turbulence, shocks).
- High order approximations are more accurate per unknown.
- High performance computing on many-core architectures (efficient explicit time-stepping).

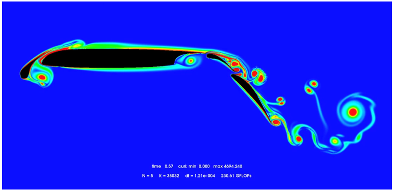

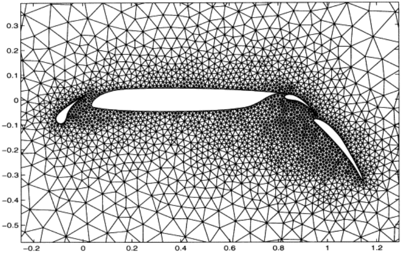

Mesh from Slawig 2001.

High order finite element methods for hyperbolic PDEs

- Focus: high accuracy in computational mechanics on unstructured meshes.
- Applications in aerodynamics (acoustics, vorticular flows, turbulence, shocks).
- High order approximations are more accurate per unknown.
- High performance computing on many-core architectures (efficient explicit time-stepping).

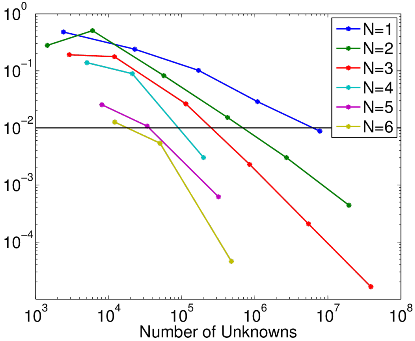

For smooth solutions, high order methods deliver a lower error per degree of freedom.

High order finite element methods for hyperbolic PDEs

- Focus: high accuracy in computational mechanics on unstructured meshes.
- Applications in aerodynamics (acoustics, vorticular flows, turbulence, shocks).
- High order approximations are more accurate per unknown.
- High performance computing on many-core architectures (efficient explicit time-stepping).

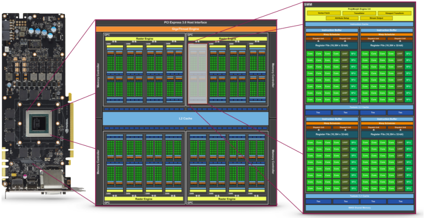

Schematic of an NVIDIA graphics processing unit (GPU).

Finite element methods: general unstructured meshes

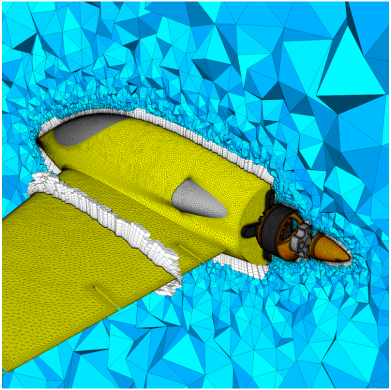

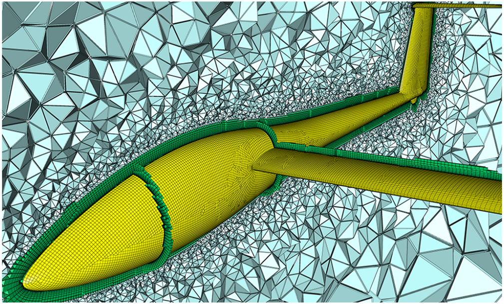

DG methods are compatible with unstructured meshes containing different types of elements (tetrahedra, hexahedra most common, but also prisms and pyramids).

Figures courtesy of Pointwise Inc (https://www.pointwise.com).

High order decreases numerical dissipation

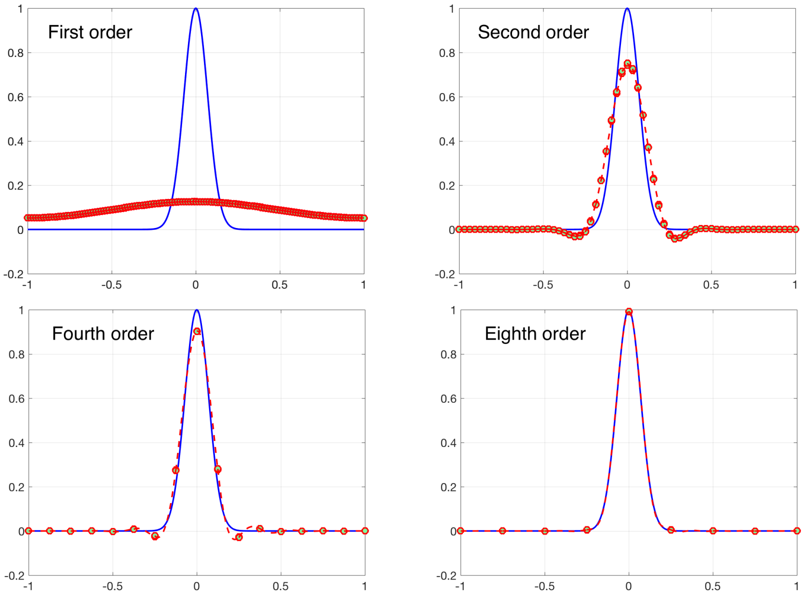

High order decreases numerical dissipation

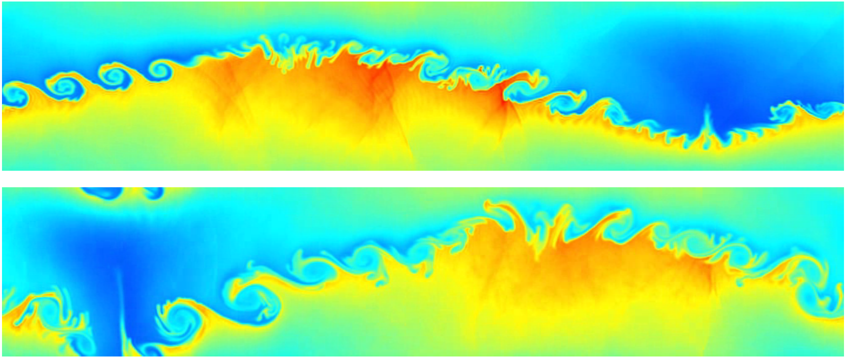

8th order simulation of forced Kelvin-Helmholtz instability (Per-Olof Persson).
Vorticular structures and acoustic forcing are both sensitive to numerical dissipation.

Talk outline

1. Stability of DG: linear PDEs vs nonlinear conservation laws
2. Summation by parts finite differences
3. High order DG and summation by parts
4. Entropy stable formulations and flux differencing
5. Numerical experiments
   - Triangular and tetrahedral meshes
   - Quadrilateral and hexahedral meshes

Talk outline

Basics of discontinuous Galerkin methods

Discontinuous Galerkin (DG) methods:

- High order accuracy, geometric flexibility.
- Weak continuity across faces.

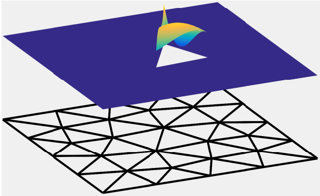

- Continuous PDE (example: advection)

$$\frac{\partial u}{\partial t} = \frac{\partial f(u)}{\partial x}, \qquad f(u) = u.$$

- Local DG form with numerical flux $\boldsymbol{f}^*$: find $u \in P^N\left(D^k\right)$ such that

$$\int_{D_k} \frac{\partial u}{\partial t}\phi = \int_{D_k} \frac{\partial f(u)}{\partial x}\phi + \int_{\partial D_k} \boldsymbol{n} \cdot \left(\boldsymbol{f}^* - \boldsymbol{f}(u)\right)\phi, \qquad \forall \phi \in P^N\left(D^k\right).$$

Basics of discontinuous Galerkin methods

Discontinuous Galerkin (DG) methods:

- High order accuracy, geometric flexibility.
- Weak continuity across faces.

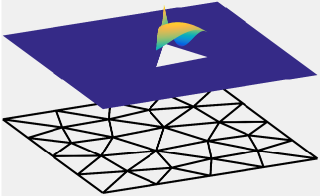

DG in space yields system of ODEs

$$\mathbf{M}_{\Omega}\frac{\mathrm{d}\mathbf{u}}{\mathrm{d}t} = \mathbf{A}\mathbf{u}.$$

DG mass matrix decouples across elements, inter-element coupling only through $\mathbf{A}$.

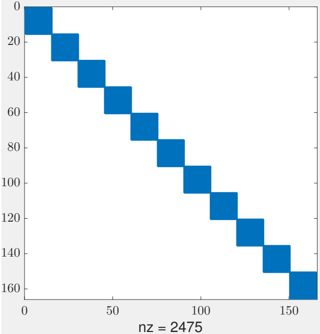

Implementation of explicit time-domain DG methods

Given initial condition $u(\mathbf{x}, 0)$:

- Compute numerical flux on element faces (non-local).
- Compute RHS of (local) ODE.
- Evolve (local) solution using explicit time integration (RK, AB, etc).

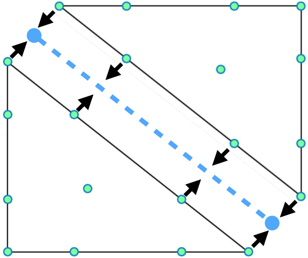

$$\frac{\mathrm{d}\mathbf{u}}{\mathrm{d}t} = \mathbf{D}_x\mathbf{u} + \sum_{\text{faces}} \mathbf{L}_f\left(\text{flux}\right), \qquad \mathbf{L}_f = \mathbf{M}^{-1}\mathbf{M}_f.$$

Implementation of explicit time-domain DG methods

Given initial condition $u(\mathbf{x}, 0)$:

- Compute numerical flux on element faces (non-local).
- Compute RHS of (local) ODE.
- Evolve (local) solution using explicit time integration (RK, AB, etc).

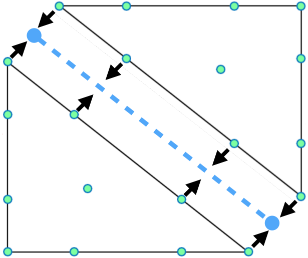

$$\frac{\mathrm{d}\mathbf{u}}{\mathrm{d}t} = \underbrace{\mathbf{D}_x \mathbf{u}}_{\text{Volume}} + \underbrace{\sum_{\text{faces}} \mathbf{L}_f \left(\text{flux}\right)}_{\text{Surface}}, \qquad \mathbf{L}_f = \mathbf{M}^{-1}\mathbf{M}_f.$$

Implementation of explicit time-domain DG methods

Given initial condition $u(\mathbf{x}, 0)$:

- Compute numerical flux on element faces (non-local).
- Compute RHS of (local) ODE.
- Evolve (local) solution using explicit time integration (RK, AB, etc).

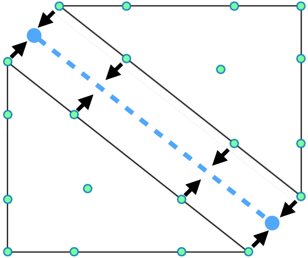

$$\underbrace{\frac{\mathrm{d}\mathbf{u}}{\mathrm{d}t}}_{\text{Update}} = \underbrace{\mathbf{D}_x \mathbf{u}}_{\text{Volume}} + \underbrace{\sum_{\text{faces}} \mathbf{L}_f \,(\text{flux})}_{\text{Surface}}, \qquad \mathbf{L}_f = \mathbf{M}^{-1}\mathbf{M}_f.$$

Implementation of explicit time-domain DG methods

Given initial condition $u(\mathbf{x}, 0)$:

- Compute numerical flux on element faces (non-local).
- Compute RHS of (local) ODE.
- Evolve (local) solution using explicit time integration (RK, AB, etc).

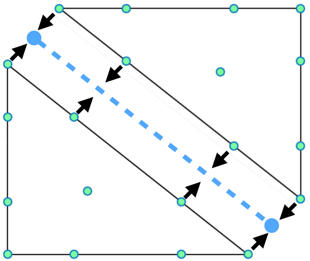

Pros: simple, scalable, and efficient matrix-free implementation.

Cons: explicit time-stepping, high order methods prone to instability. Regularization (slope limiting, artificial viscosity) to avoid blow up!

Must ensure semi-discrete system is inherently *energy stable*!

DG is semi-discretely energy stable for linear advection

- Linear periodic advection on $[-1,1]$

$$\frac{\partial u}{\partial t} + \frac{\partial u}{\partial x} = 0, \qquad u(-1) = u(1), \qquad \Longrightarrow \frac{\partial}{\partial t}\left\|u\right\|^2_{L^2([-1,1])} = 0.$$

- Triangulate domain with elements D^k, define $[\![u]\!] = u^+ - u$ on D^k.
- DG formulation: find $u(x) \in P^N(D^k)$ s.t. $\forall v \in P^N(D^k)$

$$\sum_k \int_{D^k} \left(\frac{\partial u}{\partial t} + \frac{\partial u}{\partial x}\right) v \, \mathrm{d}x + \frac{1}{2}\int_{\partial D^k} \left([\![u]\!]\, n_x + \tau\, [\![u]\!]\right) v \, \mathrm{d}x = 0.$$

- Energy estimate: take $v = u$, chain rule in time, integrate by parts.

$$\sum_k \frac{\partial}{\partial t}\left\|u\right\|^2_{D^k} \leq -\sum_k \frac{\tau}{2}\int_{\partial D^k} [\![u]\!]^2 \, \mathrm{d}x.$$

DG is semi-discretely energy stable for linear advection

- Linear periodic advection on $[-1, 1]$

$$\frac{\partial u}{\partial t} + \frac{\partial u}{\partial x} = 0, \qquad u(-1) = u(1), \qquad \Longrightarrow \frac{\partial}{\partial t} \|u\|^2_{L^2([-1,1])} = 0.$$

- Triangulate domain with elements D^k, define $[\![u]\!] = u^+ - u$ on D^k.
- DG formulation: find $u(x) \in P^N(D^k)$ s.t. $\forall v \in P^N(D^k)$

$$\sum_k \int_{D^k} \left(\frac{\partial u}{\partial t} + \frac{\partial u}{\partial x} \right) v \, \mathrm{d}x + \frac{1}{2} \int_{\partial D^k} \left([\![u]\!] \, n_x + \tau [\![u]\!] \right) v \, \mathrm{d}x = 0.$$

- Energy estimate: take $v = u$, chain rule in time, integrate by parts.

$$\sum_k \frac{\partial}{\partial t} \|u\|^2_{D^k} \leq -\sum_k \frac{\tau}{2} \int_{\partial D^k} [\![u]\!]^2 \, \mathrm{d}x.$$

DG is semi-discretely energy stable for linear advection

- Linear periodic advection on $[-1,1]$

$$\frac{\partial u}{\partial t} + \frac{\partial u}{\partial x} = 0, \qquad u(-1) = u(1), \qquad \Longrightarrow \frac{\partial}{\partial t}\left\|u\right\|^2_{L^2([-1,1])} = 0.$$

- Triangulate domain with elements D^k, define $[\![u]\!] = u^+ - u$ on D^k.
- DG formulation: find $u(x) \in P^N(D^k)$ s.t. $\forall v \in P^N(D^k)$

$$\sum_k \int_{D^k} \left(\frac{\partial u}{\partial t} + \frac{\partial u}{\partial x}\right) v \, \mathrm{d}x + \frac{1}{2}\int_{\partial D^k} \left([\![u]\!]\, n_x + \tau\, [\![u]\!]\right) v \, \mathrm{d}x = 0.$$

- Energy estimate: take $v = u$, chain rule in time, integrate by parts.

$$\sum_k \frac{\partial}{\partial t}\left\|u\right\|^2_{D^k} \leq -\sum_k \frac{\tau}{2}\int_{\partial D^k} [\![u]\!]^2 \, \mathrm{d}x.$$

Energy conservative vs. energy stable DG methods

- Energy estimate: implies solution is non-increasing if $\tau \geq 0$.
- Energy conservative (non-dissipative) "central" flux when $\tau = 0$.
- Energy stable (dissipative) "Lax-Friedrichs" flux when $\tau = 1$.

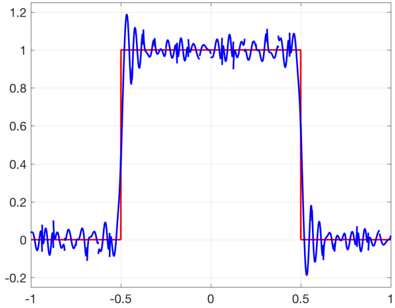

(a) Energy conservative ($\tau = 0$)

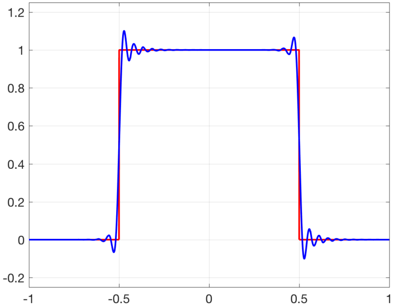

(b) Energy stable ($\tau = 1$)

Generalization to nonlinear problems: entropy stability

- Generalizes energy stability to nonlinear systems of conservation laws (Burgers', shallow water, compressible Euler, MHD).

$$\frac{\partial \boldsymbol{u}}{\partial t} + \frac{\partial \boldsymbol{f}(\boldsymbol{u})}{\partial x} = 0.$$

- Continuous entropy inequality: convex entropy function $S(\boldsymbol{u})$ and "entropy potential" $\psi(\boldsymbol{u})$.

$$\int_\Omega \boldsymbol{v}^T \left(\frac{\partial \boldsymbol{u}}{\partial t} + \frac{\partial \boldsymbol{f}(\boldsymbol{u})}{\partial x} \right) = 0, \qquad \boldsymbol{v} = \frac{\partial S}{\partial \boldsymbol{u}}$$
$$\Longrightarrow \int_\Omega \frac{\partial S(\boldsymbol{u})}{\partial t} + \left(\boldsymbol{v}^T \boldsymbol{f}(\boldsymbol{u}) - \psi(\boldsymbol{u}) \right)\Big|_{-1}^{1} \leq 0.$$

- Proof of entropy inequality relies on chain rule, integration by parts.

Example: compressible flow and mathematical entropy

- Conservative variables: density, momentum, energy

$$\boldsymbol{u} = (\rho, \boldsymbol{m}, E), \qquad \rho > 0, \qquad E > \frac{1}{2}|\boldsymbol{m}|^2/\rho.$$

- Physical entropy $s(\boldsymbol{u})$ always increasing; mathematical entropy $S(\boldsymbol{u})$ always decreasing (analogous to energy).

$$s(\boldsymbol{u}) = \log\left(\frac{(\gamma-1)\rho e}{\rho^\gamma}\right), \qquad S(\boldsymbol{u}) = -\rho s(\boldsymbol{u}).$$

- Entropy variables $\boldsymbol{v}(\boldsymbol{u})$: invertible function of $\boldsymbol{u}$

$$\boldsymbol{v}(\boldsymbol{u}) = \frac{\partial S}{\partial \boldsymbol{u}} = \frac{1}{\rho e}\begin{pmatrix} \rho e(\gamma + 1 - s(\boldsymbol{u})) - E \\ m \\ -\rho \end{pmatrix}$$

Why are discretizations of nonlinear PDEs unstable?

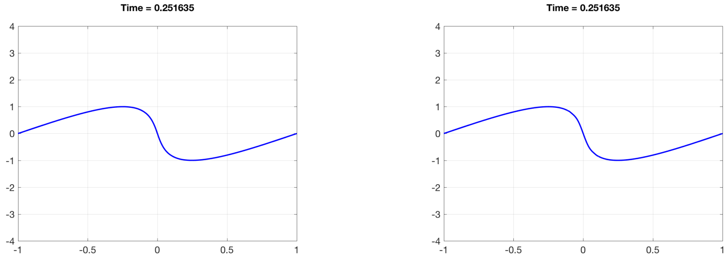

(a) $N = 7, K = 8$ (aligned mesh) (b) $N = 7, K = 9$ (non-aligned mesh)

- Burgers' equation: $f(u) = u^2/2$. How to compute $\frac{\partial}{\partial x} f(u)$?

$$\frac{\partial u}{\partial t} + \frac{1}{2}\frac{\partial u^2}{\partial x} = 0, \qquad u \in P^N(D^k), \quad u^2 \notin P^N(D^k).$$

- Differentiating L^2 projection P_N + inexact quadrature: no chain rule.

$$\int_{D^k} \left(\frac{\partial u}{\partial t} + \frac{1}{2}\frac{\partial}{\partial x} P_N u^2 \right) v \, \mathrm{d}x = 0, \qquad \frac{1}{2}\frac{\partial P_N u^2}{\partial x} \neq P_N \left(u \frac{\partial u}{\partial x} \right)$$

Why are discretizations of nonlinear PDEs unstable?

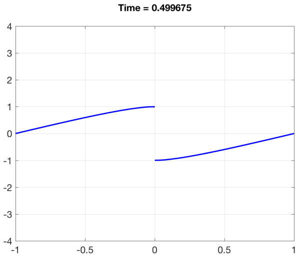

(a) $N = 7, K = 8$ (aligned mesh)

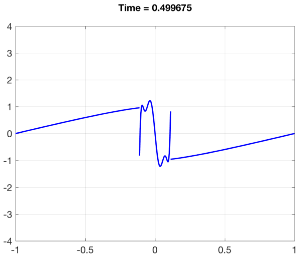

(b) $N = 7, K = 9$ (non-aligned mesh)

- Burgers' equation: $f(u) = u^2/2$. How to compute $\frac{\partial}{\partial x} f(u)$?

$$\frac{\partial u}{\partial t} + \frac{1}{2}\frac{\partial u^2}{\partial x} = 0, \qquad u \in P^N(D^k), \quad u^2 \notin P^N(D^k).$$

- Differentiating L^2 projection P_N + inexact quadrature: no chain rule.

$$\int_{D^k} \left(\frac{\partial u}{\partial t} + \frac{1}{2}\frac{\partial}{\partial x} P_N u^2 \right) v \, \mathrm{d}x = 0, \qquad \frac{1}{2}\frac{\partial P_N u^2}{\partial x} \neq P_N \left(u \frac{\partial u}{\partial x} \right)$$

Why are discretizations of nonlinear PDEs unstable?

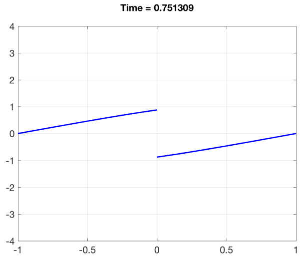

(a) $N = 7, K = 8$ (aligned mesh)

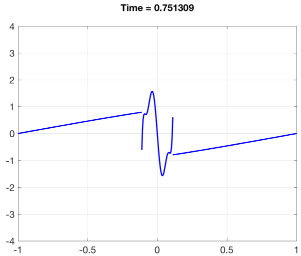

(b) $N = 7, K = 9$ (non-aligned mesh)

- Burgers' equation: $f(u) = u^2/2$. How to compute $\frac{\partial}{\partial x} f(u)$?

$$\frac{\partial u}{\partial t} + \frac{1}{2}\frac{\partial u^2}{\partial x} = 0, \qquad u \in P^N(D^k), \quad u^2 \notin P^N(D^k).$$

- Differentiating L^2 projection P_N + inexact quadrature: no chain rule.

$$\int_{D^k} \left(\frac{\partial u}{\partial t} + \frac{1}{2}\frac{\partial}{\partial x} P_N u^2 \right) v \,\mathrm{d}x = 0, \qquad \frac{1}{2}\frac{\partial P_N u^2}{\partial x} \neq P_N\left(u \frac{\partial u}{\partial x} \right)$$

Why are discretizations of nonlinear PDEs unstable?

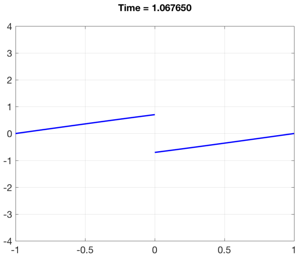

(a) $N=7, K=8$ (aligned mesh)

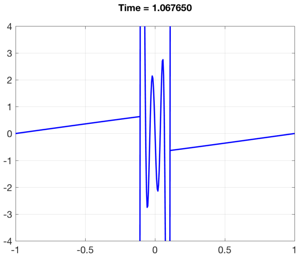

(b) $N=7, K=9$ (non-aligned mesh)

- Burgers' equation: $f(u)=u^2/2$. How to compute $\frac{\partial}{\partial x} f(u)$?

$$\frac{\partial u}{\partial t}+\frac{1}{2}\frac{\partial u^2}{\partial x}=0, \qquad u \in P^N(D^k), \quad u^2 \notin P^N(D^k).$$

- Differentiating L^2 projection P_N + inexact quadrature: no chain rule.

$$\int_{D^k}\left(\frac{\partial u}{\partial t}+\frac{1}{2}\frac{\partial}{\partial x}P_N u^2\right) v \,\mathrm{d}x = 0, \qquad \frac{1}{2}\frac{\partial P_N u^2}{\partial x} \neq P_N\left(u\frac{\partial u}{\partial x}\right)$$

Tradeoff: high order accuracy vs stability

- Asymptotic stability for smooth solutions (not shocks or turbulence!)
- Common fix: stabilize by regularizing (limiters, filters, art. viscosity).

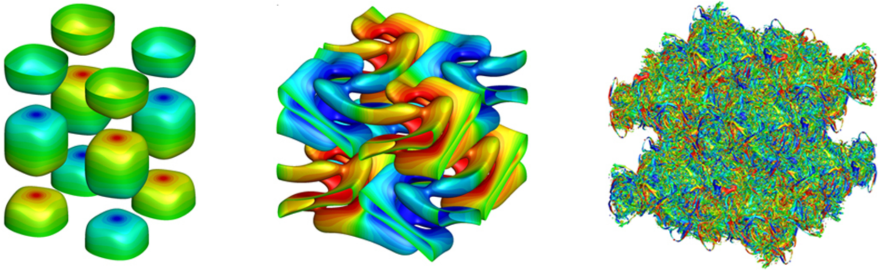

Under-resolved solutions: turbulence (inviscid Taylor-Green vortex).

Figures courtesy of Gregor Gassner, T. Warburton, Coastal Inlets Research Program (CIRP), "Man on Wire" (2008).

Tradeoff: high order accuracy vs stability

- Asymptotic stability for smooth solutions (not shocks or turbulence!)
- Common fix: stabilize by regularizing (limiters, filters, art. viscosity).

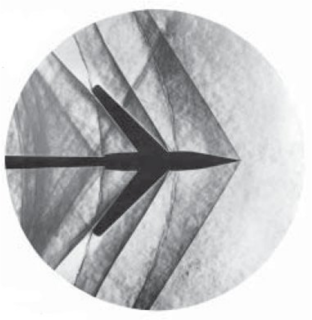

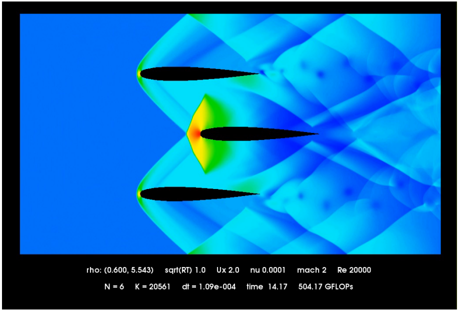

Under-resolved solutions: shock waves.

Figures courtesy of Gregor Gassner, T. Warburton, Coastal Inlets Research Program (CIRP), "Man on Wire" (2008).

Tradeoff: high order accuracy vs stability

- Asymptotic stability for smooth solutions (not shocks or turbulence!)
- Common fix: stabilize by regularizing (limiters, filters, art. viscosity).

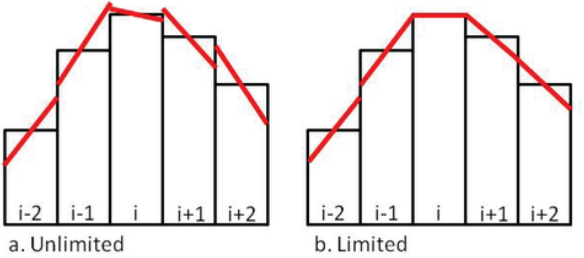

Slope limiting for a finite volume method.

Figures courtesy of Gregor Gassner, T. Warburton, Coastal Inlets Research Program (CIRP), "Man on Wire" (2008).

Tradeoff: high order accuracy vs stability

- Asymptotic stability for smooth solutions (not shocks or turbulence!)
- Common fix: stabilize by regularizing (limiters, filters, art. viscosity).

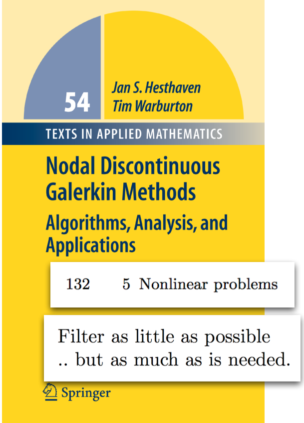

Figures courtesy of Gregor Gassner, T. Warburton, Coastal Inlets Research Program (CIRP), "Man on Wire" (2008).

Tradeoff: high order accuracy vs stability

- Asymptotic stability for smooth solutions (not shocks or turbulence!)
- Common fix: stabilize by regularizing (limiters, filters, art. viscosity).

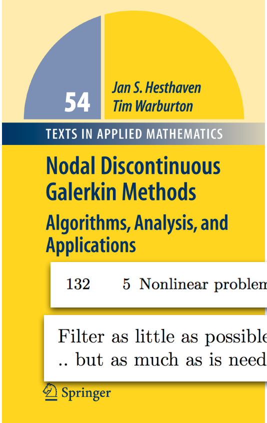

132 5 Nonlinear problems

Filter as little as possible
.. but as much as is needed.

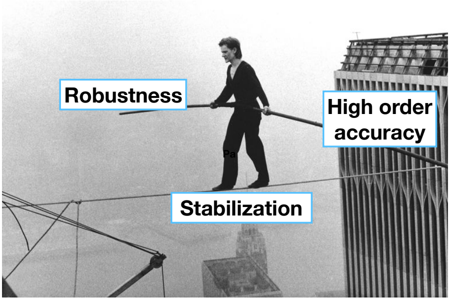

Figures courtesy of Gregor Gassner, T. Warburton, Coastal Inlets Research Program (CIRP), "Man on Wire" (2008).

Talk outline

Summation-by-parts (SBP) finite differences

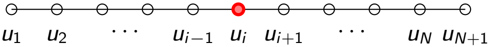

Simplest SBP finite difference matrix: combine 2nd order finite difference formulas at interior points with 1st order finite differences at boundary points .

$$\left.\frac{\partial u}{\partial x}\right|_{x=x_i} \approx \frac{u_{i+1}-u_{i-1}}{2\Delta x} \qquad \text{(at interior points } x_i\text{)},$$

$$\boldsymbol{D} = \frac{1}{2\Delta x}\begin{bmatrix} {\color{red}?} & {\color{red}?} & & \\ -1 & 0 & 1 & \\ & -1 & 0 & \ddots \\ & & \ddots & \ddots \end{bmatrix}, \qquad \boldsymbol{M} = \Delta x \begin{bmatrix} {\color{red}?} & & & \\ & 1 & & \\ & & 1 & \\ & & & \ddots \end{bmatrix}.$$

Summation-by-parts (SBP) finite differences

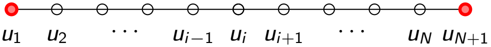

Simplest SBP finite difference matrix: combine 2nd order finite difference formulas at interior points with 1st order finite differences at boundary points .

$$\left.\frac{\partial u}{\partial x}\right|_{x=x_i} \approx \frac{u_2 - u_1}{\Delta x}, \qquad \frac{u_{N+1} - u_N}{\Delta x} \qquad \text{(at boundary pts } x_i\text{)}$$

$$\boldsymbol{D} = \frac{1}{2\Delta x}\begin{bmatrix} -2 & 2 & & \\ -1 & 0 & 1 & \\ & -1 & 0 & \ddots \\ & & \ddots & \ddots \end{bmatrix}, \qquad \boldsymbol{M} = \Delta x \begin{bmatrix} 1/2 & & & \\ & 1 & & \\ & & 1 & \\ & & & \ddots \end{bmatrix}.$$

Summation-by-parts (SBP) finite differences

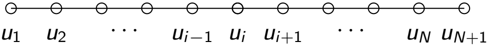

Simplest SBP finite difference matrix: combine 2nd order finite difference formulas at interior points with 1st order finite differences at boundary points .

$$\boldsymbol{MD} = \frac{1}{2}\begin{bmatrix} -1 & 1 & & \\ -1 & 0 & 1 & \\ & -1 & 0 & \ddots \\ & & \ddots & \ddots \end{bmatrix}, \qquad \boldsymbol{MD} + \boldsymbol{D}^T\boldsymbol{M} = \underbrace{\begin{bmatrix} -1 & & & \\ & 0 & & \\ & & \ddots & \\ & & & 1 \end{bmatrix}}_{\boldsymbol{B}}.$$

Semi-discrete stability for SBP finite differences

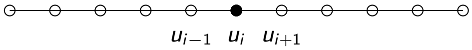

- Mimic integration by parts: difference matrix $\boldsymbol{D}$, "norm" matrix $\boldsymbol{M}$

$$\boldsymbol{MD} = \boldsymbol{B} - \boldsymbol{D}^T\boldsymbol{M}, \qquad \boldsymbol{M} \text{ diagonal, pos-def.}$$

- Discretize advection using $\boldsymbol{D}$ + weak periodic boundary conditions

$$\frac{\mathrm{d}\boldsymbol{u}}{\mathrm{d}t} + \boldsymbol{Du} + \frac{1}{\Delta x}\begin{bmatrix} -\left(u_N - u_1\right) \\ \vdots \\ \left(u_1 - u_N\right) \end{bmatrix} = \boldsymbol{0}.$$

- Multiply by $\boldsymbol{u}^T\boldsymbol{M}$, use chain rule in time + SBP property to get

$$\frac{1}{2}\frac{\mathrm{d}}{\mathrm{d}t}\boldsymbol{u}^T\boldsymbol{Mu} = 0 \Longrightarrow \text{ semi-discrete stability!}$$

Higher order SBP approximations

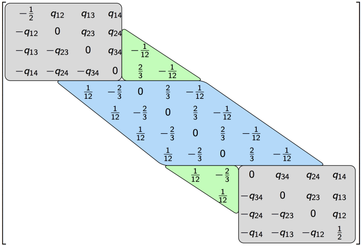

(a) 1D matrix ($N = 2$, equispaced)

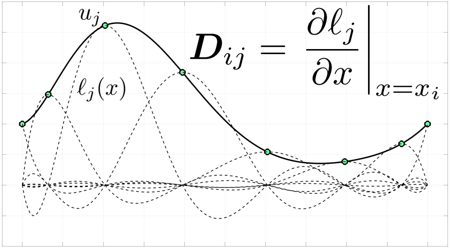

(b) 1D SBP ($N = 7$, GLL nodes)

- Can construct higher order SBP finite difference matrices.
- Explicit construction of SBP matrices from an interpolatory polynomial basis + Gauss-Legendre-Lobatto quadrature.

Figure courtesy of David C. Del Rey Fernandez.

Fisher and Carpenter (2013). *High-order ES finite difference schemes for nonlinear conservation laws: Finite domains.*

Gassner, Winters, and Kopriva (2016). *Split form nodal DG schemes with SBP property for the comp. Euler equations.*

Summary of entropy stable schemes

- Traditional SBP scheme (unstable), ignoring boundary conditions:

$$\frac{\mathrm{d}\boldsymbol{u}}{\mathrm{d}t} + \boldsymbol{D}\boldsymbol{f}(\boldsymbol{u}) = 0 \quad \Longrightarrow \quad \frac{\mathrm{d}\boldsymbol{u}_i}{\mathrm{d}t} + \sum_j \boldsymbol{D}_{ij}\boldsymbol{f}(\boldsymbol{u}_i) = 0.$$

- "Entropy conservative" finite volume numerical flux $\boldsymbol{f}_S(\boldsymbol{u}_L, \boldsymbol{u}_R)$.
- Flux differencing: $\boldsymbol{f}_S(\boldsymbol{u}_i, \boldsymbol{u}_j) = \frac{1}{2}(\boldsymbol{u}_i + \boldsymbol{u}_j)$ recovers traditional scheme.

$$\frac{\mathrm{d}\boldsymbol{u}_i}{\mathrm{d}t} + \sum_j \boldsymbol{D}_{ij} 2\boldsymbol{f}_S(\boldsymbol{u}_i, \boldsymbol{u}_j) = 0 \quad \Longrightarrow \quad \frac{\mathrm{d}\boldsymbol{u}}{\mathrm{d}t} + 2(\boldsymbol{D} \circ \boldsymbol{F}_S)\mathbf{1} = 0.$$

- Semi-discrete entropy equality using SBP (modify for inequality)

$$\boldsymbol{M}\frac{\mathrm{d}S(\boldsymbol{u})}{\mathrm{d}t} + \mathbf{1}^T\boldsymbol{B}\left(\boldsymbol{v}^T\boldsymbol{f}(\boldsymbol{u}) - \psi(\boldsymbol{u})\right) = 0.$$

Summary of entropy stable schemes

- Traditional SBP scheme (unstable), ignoring boundary conditions:

$$\frac{\mathrm{d}\boldsymbol{u}}{\mathrm{d}t} + \boldsymbol{D}\boldsymbol{f}(\boldsymbol{u}) = 0 \quad \Longrightarrow \quad \frac{\mathrm{d}\boldsymbol{u}_i}{\mathrm{d}t} + \sum_j \boldsymbol{D}_{ij}\boldsymbol{f}\left(\boldsymbol{u}_i\right) = 0.$$

- "Entropy conservative" finite volume numerical flux $\boldsymbol{f}_S(\boldsymbol{u}_L, \boldsymbol{u}_R)$.

- Flux differencing: $\boldsymbol{f}_S(\boldsymbol{u}_i, \boldsymbol{u}_j) = \frac{1}{2}\left(\boldsymbol{u}_i + \boldsymbol{u}_j\right)$ recovers traditional scheme.

$$\frac{\mathrm{d}\boldsymbol{u}_i}{\mathrm{d}t} + \sum_j \boldsymbol{D}_{ij} 2\boldsymbol{f}_S\left(\boldsymbol{u}_i, \boldsymbol{u}_j\right) = 0 \quad \Longrightarrow \quad \frac{\mathrm{d}\boldsymbol{u}}{\mathrm{d}t} + 2\left(\boldsymbol{D} \circ \boldsymbol{F}_S\right)\boldsymbol{1} = 0.$$

- Semi-discrete entropy equality using SBP (modify for inequality)

$$\boldsymbol{M}\frac{\mathrm{d}S(\boldsymbol{u})}{\mathrm{d}t} + \boldsymbol{1}^T\boldsymbol{B}\left(\boldsymbol{v}^T\boldsymbol{f}(\boldsymbol{u}) - \psi(\boldsymbol{u})\right) = 0.$$

Summary of entropy stable schemes

- Traditional SBP scheme (unstable), ignoring boundary conditions:

$$\frac{\mathrm{d}\boldsymbol{u}}{\mathrm{d}t} + \boldsymbol{D}\boldsymbol{f}(\boldsymbol{u}) = 0 \quad \Longrightarrow \quad \frac{\mathrm{d}\boldsymbol{u}_i}{\mathrm{d}t} + \sum_j \boldsymbol{D}_{ij}\boldsymbol{f}\left(\boldsymbol{u}_i\right) = 0.$$

- "Entropy conservative" finite volume numerical flux $\boldsymbol{f}_S(\boldsymbol{u}_L, \boldsymbol{u}_R)$.
- Flux differencing: $\boldsymbol{f}_S(\boldsymbol{u}_i, \boldsymbol{u}_j) = \frac{1}{2}\left(\boldsymbol{u}_i + \boldsymbol{u}_j\right)$ recovers traditional scheme.

$$\frac{\mathrm{d}\boldsymbol{u}_i}{\mathrm{d}t} + \sum_j \boldsymbol{D}_{ij} 2\boldsymbol{f}_S\left(\boldsymbol{u}_i, \boldsymbol{u}_j\right) = 0 \quad \Longrightarrow \quad \frac{\mathrm{d}\boldsymbol{u}}{\mathrm{d}t} + 2\left(\boldsymbol{D} \circ \boldsymbol{F}_S\right)\boldsymbol{1} = 0.$$

- Semi-discrete entropy equality using SBP (modify for inequality)

$$\boldsymbol{M}\frac{\mathrm{d}S(\boldsymbol{u})}{\mathrm{d}t} + \boldsymbol{1}^T\boldsymbol{B}\left(\boldsymbol{v}^T\boldsymbol{f}(\boldsymbol{u}) - \psi(\boldsymbol{u})\right) = 0.$$

Summary of entropy stable schemes

- Traditional SBP scheme (unstable), ignoring boundary conditions:

$$\frac{\mathrm{d}\boldsymbol{u}}{\mathrm{d}t} + \boldsymbol{D}\boldsymbol{f}(\boldsymbol{u}) = 0 \quad \Longrightarrow \quad \frac{\mathrm{d}\boldsymbol{u}_i}{\mathrm{d}t} + \sum_j \boldsymbol{D}_{ij}\boldsymbol{f}(\boldsymbol{u}_i) = 0.$$

- "Entropy conservative" finite volume numerical flux $\boldsymbol{f}_S(\boldsymbol{u}_L, \boldsymbol{u}_R)$.
- Flux differencing: $\boldsymbol{f}_S(\boldsymbol{u}_i, \boldsymbol{u}_j) = \frac{1}{2}(\boldsymbol{u}_i + \boldsymbol{u}_j)$ recovers traditional scheme.

$$\frac{\mathrm{d}\boldsymbol{u}_i}{\mathrm{d}t} + \sum_j \boldsymbol{D}_{ij} 2\boldsymbol{f}_S(\boldsymbol{u}_i, \boldsymbol{u}_j) = 0 \quad \Longrightarrow \quad \frac{\mathrm{d}\boldsymbol{u}}{\mathrm{d}t} + 2(\boldsymbol{D} \circ \boldsymbol{F}_S)\boldsymbol{1} = 0.$$

- Semi-discrete entropy equality using SBP (modify for inequality)

$$\boldsymbol{M}\frac{\mathrm{d}S(\boldsymbol{u})}{\mathrm{d}t} + \boldsymbol{1}^T\boldsymbol{B}\left(\boldsymbol{v}^T\boldsymbol{f}(\boldsymbol{u}) - \psi(\boldsymbol{u})\right) = 0.$$

Talk outline

1 Stability of DG: linear PDEs vs nonlinear conservation laws

2 Summation by parts finite differences

3 High order DG and summation by parts

4 Entropy stable formulations and flux differencing

5 Numerical experiments
- Triangular and tetrahedral meshes
- Quadrilateral and hexahedral meshes

Entropy stable SBP discretizations: current/challenges

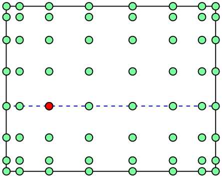

(a) GLL collocation

- (Current) Discrete entropy inequality using high order GLL hexes.
- Gauss quadrature: more accurate but expensive coupling conditions.
- Tetrahedra, wedges, pyramids? Over-integration?

Fisher and Carpenter (2013). *High-order ES finite difference schemes for nonlinear conservation laws: Finite domains.*

Carpenter et al. (2014). *Entropy stable spectral collocation schemes for the NS equations: discontinuous interfaces.*

Entropy stable SBP discretizations: current/challenges

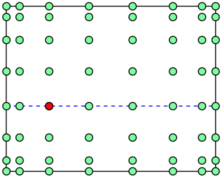

(a) GLL collocation

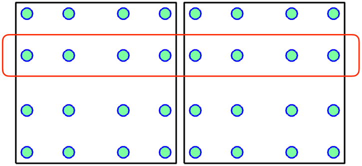

(b) Gauss nodes element coupling

- (Current) Discrete entropy inequality using high order GLL hexes.
- Gauss quadrature: more accurate but expensive coupling conditions.
- Tetrahedra, wedges, pyramids? Over-integration?

Fisher and Carpenter (2013). *High-order ES finite difference schemes for nonlinear conservation laws: Finite domains.*

Carpenter et al. (2014). *Entropy stable spectral collocation schemes for the NS equations: discontinuous interfaces.*

Entropy stable SBP discretizations: current/challenges

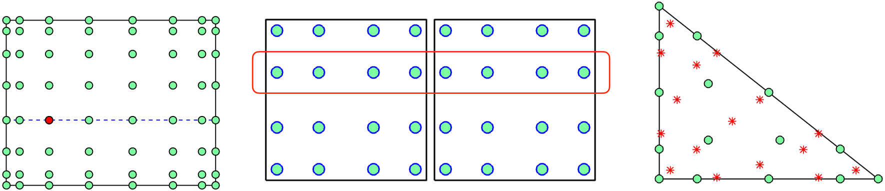

(a) GLL collocation (b) Gauss nodes element coupling (c) Nodes vs quadrature

- (Current) Discrete entropy inequality using high order GLL hexes.
- Gauss quadrature: more accurate but expensive coupling conditions.
- Tetrahedra, wedges, pyramids? Over-integration?

Fisher and Carpenter (2013). *High-order ES finite difference schemes for nonlinear conservation laws: Finite domains.*

Carpenter et al. (2014). *Entropy stable spectral collocation schemes for the NS equations: discontinuous interfaces.*

Entropy stable SBP discretizations: current/challenges

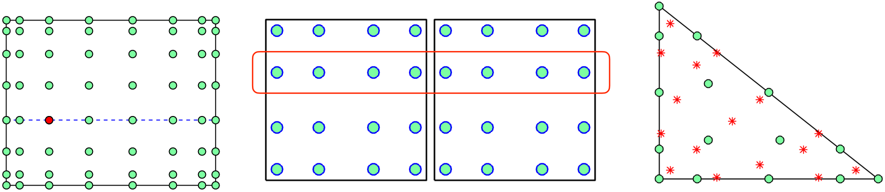

(a) GLL collocation (b) Gauss nodes element coupling (c) Nodes vs quadrature

- (Current) Discrete entropy inequality using high order GLL hexes.
- Gauss quadrature: more accurate but expensive coupling conditions.
- Tetrahedra, wedges, pyramids? Over-integration?

Goal: entropy stable high order DG with compact stencils using arbitrary basis functions and volume/surface quadrature points.

Fisher and Carpenter (2013). *High-order ES finite difference schemes for nonlinear conservation laws: Finite domains.*
Carpenter et al. (2014). *Entropy stable spectral collocation schemes for the NS equations: discontinuous interfaces.*

Quadrature-based matrices for polynomial bases

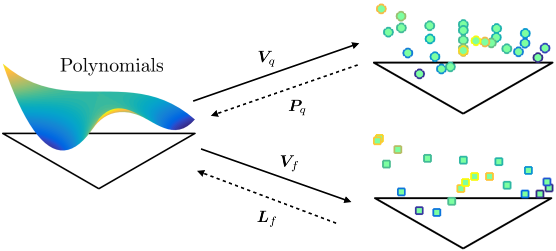

- Assume degree $2N$ volume, surface quadratures $(\boldsymbol{x}_i^q, \boldsymbol{w}_i^q)$, $(\boldsymbol{x}_i^f, \boldsymbol{w}_i^f)$, and basis $\phi_1, \ldots, \phi_{N_p}$. Define interpolation matrices $\boldsymbol{V}_q$, $\boldsymbol{V}_f$

$$(\boldsymbol{V}_q)_{ij} = \phi_j(\boldsymbol{x}_i^q), \qquad (\boldsymbol{V}_f)_{ij} = \phi_j(\boldsymbol{x}_i^f).$$

- Introduce quadrature-based L^2 projection and lifting matrices

$$\boldsymbol{P}_q = \boldsymbol{M}^{-1}\boldsymbol{V}_q^T\boldsymbol{W}, \qquad \boldsymbol{L}_f = \boldsymbol{M}^{-1}\boldsymbol{V}_f^T\boldsymbol{W}_f,$$
$$\boldsymbol{W} = \operatorname{diag}(\boldsymbol{w}^q), \qquad \boldsymbol{W}_f = \operatorname{diag}\left(\boldsymbol{w}^f\right).$$

Quadrature-based differentiation matrices

- Matrix $\boldsymbol{D}_q^i$: evaluates derivative of L^2 projection at points $\boldsymbol{x}^q$.

$$\boldsymbol{D}_q^i = \boldsymbol{V}_q \boldsymbol{D}^i \boldsymbol{P}_q, \qquad \boldsymbol{D}^i \quad \text{exactly differentiates polynomials.}$$

- Summation-by-parts involving L^2 projection:

$$\boldsymbol{W}\boldsymbol{D}_q^i + \left(\boldsymbol{W}\boldsymbol{D}_q^i\right)^T = \left(\boldsymbol{V}_f \boldsymbol{P}_q\right)^T \boldsymbol{W}_f \operatorname{diag}\left(\boldsymbol{n}_i\right) \boldsymbol{V}_f \boldsymbol{P}_q.$$

- Equivalent to integration-by-parts + quadrature: for $u, v \in L^2\left(\widehat{D}\right)$

$$\int_{\widehat{D}} \frac{\partial P_N u}{\partial x_i} v + \int_{\widehat{D}} u \frac{\partial P_N v}{\partial x_i} = \int_{\partial \widehat{D}} \left(P_N u\right)\left(P_N v\right) \widehat{n}_i$$

- Quadrature may not contain boundary points: complicated interface terms for coupling neighboring elements or imposing BCs.

A "decoupled" block SBP operator

- Approx. derivatives also using boundary traces (compact coupling).
- On an element D^k with unit normal vector $\boldsymbol{n}$: approximate derivative with respect to the ith coordinate.

$$\boldsymbol{D}_N^i = \begin{bmatrix} \boldsymbol{D}_q^i - \frac{1}{2}\boldsymbol{V}_q \boldsymbol{L}_f \operatorname{diag}(\boldsymbol{n}_i)\boldsymbol{V}_f \boldsymbol{P}_q & \frac{1}{2}\boldsymbol{V}_q \boldsymbol{L}_f \operatorname{diag}(\boldsymbol{n}_i) \\ -\frac{1}{2}\operatorname{diag}(\boldsymbol{n}_i)\boldsymbol{V}_f \boldsymbol{P}_q & \frac{1}{2}\operatorname{diag}(\boldsymbol{n}_i) \end{bmatrix},$$

- $\boldsymbol{D}_N^i$ satisfies a summation-by-parts (SBP) property

$$\boldsymbol{Q}_N^i = \begin{bmatrix} \boldsymbol{W} & \\ & \boldsymbol{W}_f \end{bmatrix} \boldsymbol{D}_N^i, \qquad \boldsymbol{B}_N = \begin{bmatrix} 0 & \\ & \boldsymbol{W}_f \boldsymbol{n}_i \end{bmatrix},$$

$$\boxed{\boldsymbol{Q}_N^i + \left(\boldsymbol{Q}_N^i\right)^T = \boldsymbol{B}_N} \sim \boxed{\int_{D^k} \frac{\partial f}{\partial x_i} g + f \frac{\partial g}{\partial x_i} = \int_{\partial D^k} f g \boldsymbol{n}_i}.$$

Decoupled SBP operators: adding boundary corrections

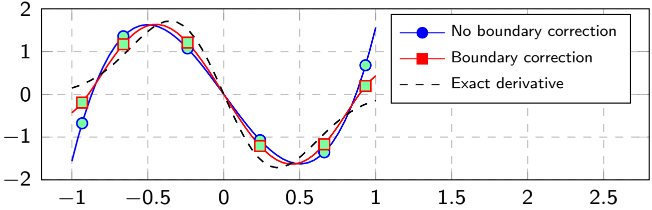

- $\boldsymbol{D}_N^i$ produces a high order approximation of $f\frac{\partial g}{\partial x}$ at $\boldsymbol{x} = [\boldsymbol{x}^q, \boldsymbol{x}^f]$.

$$f\frac{\partial g}{\partial x} \approx \begin{bmatrix} \boldsymbol{P}_q & \boldsymbol{L}_f \end{bmatrix} \operatorname{diag}(\boldsymbol{f})\, \boldsymbol{D}_N \boldsymbol{g}, \qquad \boldsymbol{f}_i, \boldsymbol{g}_i = f(\boldsymbol{x}_i), g(\boldsymbol{x}_i).$$

- Equivalent to solving a variational problem for $u(\boldsymbol{x}) \approx f\frac{\partial g}{\partial x}$ involving the L^2 projection P_N onto degree N polynomials

$$\int_{D^k} u(\boldsymbol{x})v(\boldsymbol{x}) = \int_{D^k} f\frac{\partial P_N g}{\partial x} v + \int_{\partial D^k} (f - P_N f)\frac{(gv + P_N(gv))}{2}.$$

Talk outline

Burgers' equation: energy stable formulations

- Split form of Burgers' equation

$$\frac{\partial u}{\partial t} + \frac{1}{3}\left(\frac{\partial u^2}{\partial x} + u\frac{\partial u}{\partial x}\right) = 0$$

- Stable DG method: let $u(x) = \sum_j \widehat{\boldsymbol{u}}_j \phi(x)$. Find $\widehat{\boldsymbol{u}}$ such that

$$\boldsymbol{u} = \begin{bmatrix} \boldsymbol{V}_q \\ \boldsymbol{V}_f \end{bmatrix} \widehat{\boldsymbol{u}}, \qquad \boldsymbol{f}^* = \boldsymbol{f}^*(u^+, u) = \text{numerical flux}$$

$$\frac{\mathrm{d}\widehat{\boldsymbol{u}}}{\mathrm{d}t} + \frac{1}{3}\begin{bmatrix} \boldsymbol{P}_q & \boldsymbol{L}_f \end{bmatrix}\left(\boldsymbol{D}_N\left(\boldsymbol{u}^2\right) + \operatorname{diag}\left(\boldsymbol{u}\right)\boldsymbol{D}_N\boldsymbol{u}\right) + \boldsymbol{L}_f(\boldsymbol{f}^*) = 0.$$

- Energy estimate: multiply by $\widehat{\boldsymbol{u}}^T\boldsymbol{M}$, use SBP, sum over D^k

$$\sum_k \frac{1}{2}\frac{\mathrm{d}}{\mathrm{d}t}\widehat{\boldsymbol{u}}^T\boldsymbol{M}\widehat{\boldsymbol{u}} = \sum_k \frac{1}{2}\frac{\partial}{\partial t}\left\|u\right\|^2_{L^2(D^k)} \leq 0.$$

Burgers' equation: energy stable shock solution

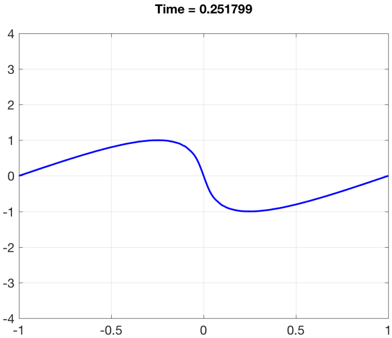

(a) $\tau = 0$

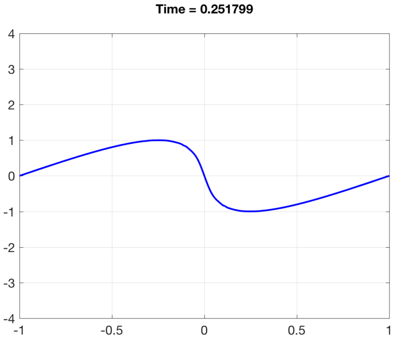

(b) $\tau = 1$

Burgers' equation: energy stable shock solution

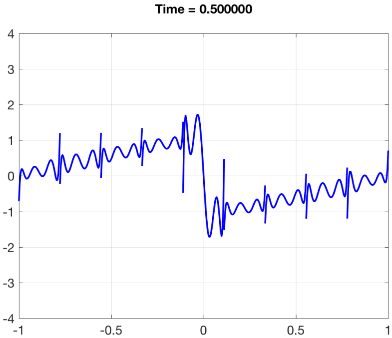

(a) $\tau = 0$

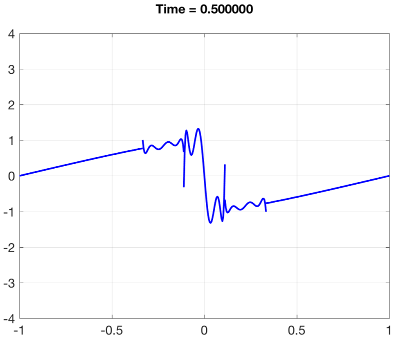

(b) $\tau = 1$

Burgers' equation: energy stable shock solution

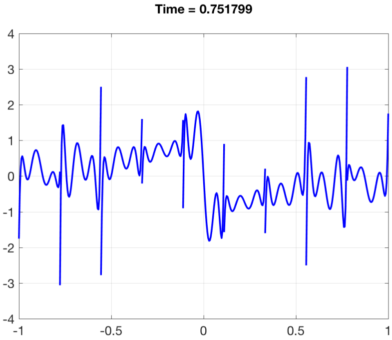

(a) $\tau = 0$

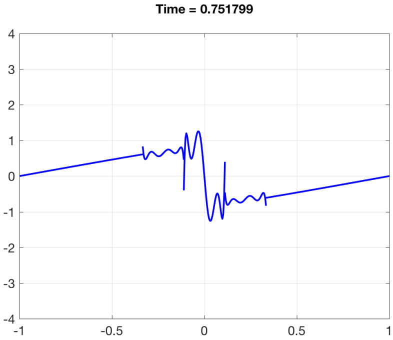

(b) $\tau = 1$

Burgers' equation: energy stable shock solution

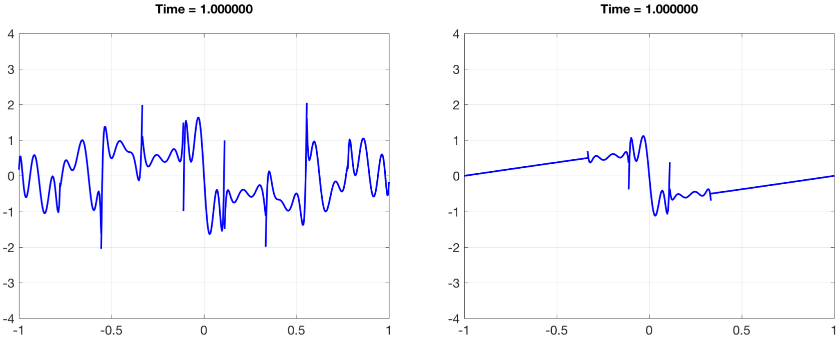

(a) $\tau = 0$ (b) $\tau = 1$

Burgers' equation: energy stable shock solution

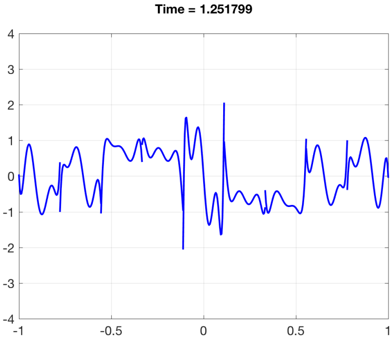

(a) $\tau = 0$

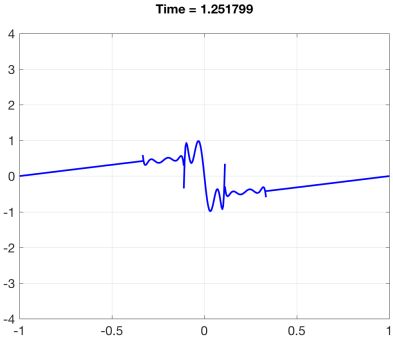

(b) $\tau = 1$

Burgers' equation: energy stable shock solution

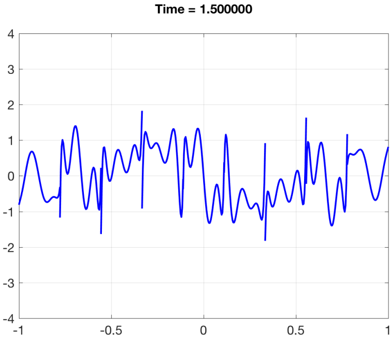

(a) $\tau = 0$

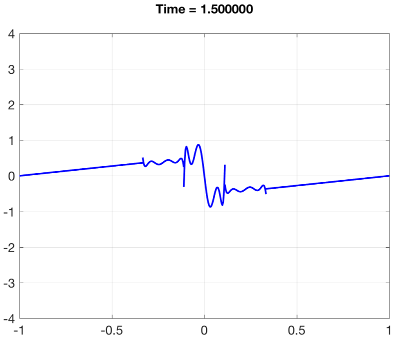

(b) $\tau = 1$

Burgers' equation: energy stable shock solution

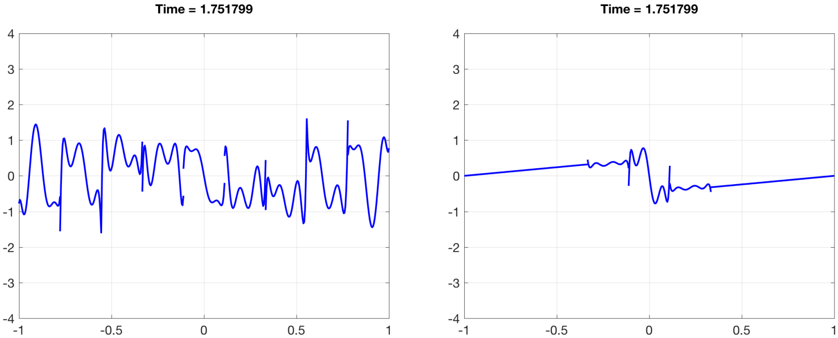

(a) $\tau = 0$ (b) $\tau = 1$

Burgers' equation: energy stable shock solution

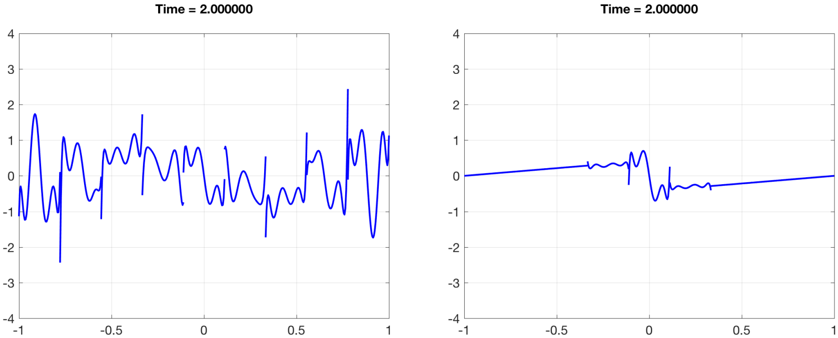

(a) $\tau = 0$ (b) $\tau = 1$

Burgers' equation: energy stable shock solution

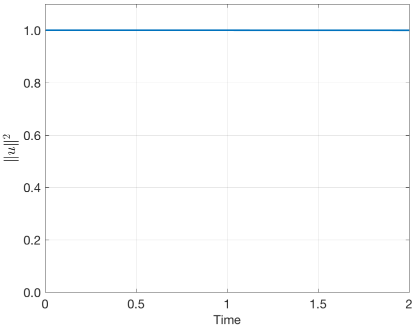

(a) Energy conservative ($\tau = 0$)

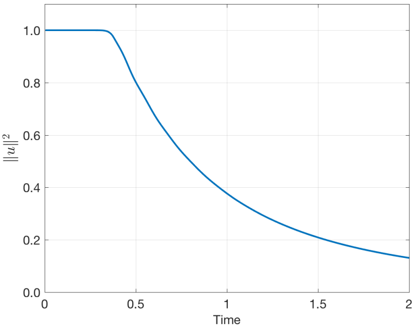

(b) Energy stable ($\tau = 1$)

Flux differencing: entropy conservative finite volume fluxes

- Tadmor's entropy conservative (mean value) numerical flux

$$\begin{aligned} \boldsymbol{f}_S(\boldsymbol{u},\boldsymbol{u}) &= \boldsymbol{f}(\boldsymbol{u}), && \text{(consistency)} \\ \boldsymbol{f}_S(\boldsymbol{u},\boldsymbol{v}) &= \boldsymbol{f}_S(\boldsymbol{v},\boldsymbol{u}), && \text{(symmetry)} \\ \left(\boldsymbol{v}_L - \boldsymbol{v}_R\right)^T \boldsymbol{f}\left(\boldsymbol{u}_L,\boldsymbol{u}_R\right) &= \psi_L - \psi_R, && \text{(conservation).} \end{aligned}$$

- Example: entropy conservative flux for Burgers' equation

$$f_S(u_L,u_R) = \frac{1}{6}\left(u_L^2 + u_L u_R + u_R^2\right).$$

- Flux differencing: using finite volume numerical fluxes to evaluate high order derivatives in DG methods.

Tadmor, Eitan (1987). *The numerical viscosity of entropy stable schemes for systems of conservation laws. I.*

Flux differencing: entropy conservative finite volume fluxes

- Tadmor's entropy conservative (mean value) numerical flux

$$\begin{aligned} \boldsymbol{f}_S(\boldsymbol{u}, \boldsymbol{u}) &= \boldsymbol{f}(\boldsymbol{u}), \qquad \text{(consistency)} \\ \boldsymbol{f}_S(\boldsymbol{u}, \boldsymbol{v}) &= \boldsymbol{f}_S(\boldsymbol{v}, \boldsymbol{u}), \qquad \text{(symmetry)} \\ (\boldsymbol{v}_L - \boldsymbol{v}_R)^T \boldsymbol{f}(\boldsymbol{u}_L, \boldsymbol{u}_R) &= \psi_L - \psi_R, \qquad \text{(conservation)}. \end{aligned}$$

- Example: entropy conservative flux for Burgers' equation

$$f_S(u_L, u_R) = \frac{1}{6}\left(u_L^2 + u_L u_R + u_R^2\right).$$

- Flux differencing: using finite volume numerical fluxes to evaluate high order derivatives in DG methods.

Tadmor, Eitan (1987). *The numerical viscosity of entropy stable schemes for systems of conservation laws. I.*

Flux differencing: entropy conservative finite volume fluxes

- Tadmor's entropy conservative (mean value) numerical flux

$$\begin{aligned} \boldsymbol{f}_S(\boldsymbol{u},\boldsymbol{u}) &= \boldsymbol{f}(\boldsymbol{u}), \qquad &\text{(consistency)}\\ \boldsymbol{f}_S(\boldsymbol{u},\boldsymbol{v}) &= \boldsymbol{f}_S(\boldsymbol{v},\boldsymbol{u}), \qquad &\text{(symmetry)}\\ (\boldsymbol{v}_L-\boldsymbol{v}_R)^T\,\boldsymbol{f}\left(\boldsymbol{u}_L,\boldsymbol{u}_R\right) &= \psi_L-\psi_R, \qquad &\text{(conservation).} \end{aligned}$$

- Example: entropy conservative flux for Burgers' equation

$$f_S(u_L,u_R) = \frac{1}{6}\left(u_L^2+u_Lu_R+u_R^2\right).$$

- Flux differencing: using finite volume numerical fluxes to evaluate high order derivatives in DG methods.

Tadmor, Eitan (1987). *The numerical viscosity of entropy stable schemes for systems of conservation laws. I.*

Flux differencing: recovering split formulations

- Entropy conservative flux for Burgers' equation

$$f_S(u_L, u_R) = \frac{1}{6}\left(u_L^2 + u_L u_R + u_R^2\right).$$

- Flux differencing: let $u_L = u(x), u_R = u(y)$

$$\frac{\partial f(u)}{\partial x} \Longrightarrow 2\left.\frac{\partial f_S\left(u(x), u(y)\right)}{\partial x}\right|_{y=x}$$

- Recovering the Burgers' split formulation

$$f_S(u(x), u(y)) = \frac{1}{6}\left(u(x)^2 + u(x)u(y) + u(y)^2\right)$$

$$2\left.\frac{\partial f_S\left(u(x), u(y)\right)}{\partial x}\right|_{y=x} = \frac{1}{3}\frac{\partial u^2}{\partial x} + \frac{1}{3}u\frac{\partial u}{\partial x} + \frac{1}{3}u^2\frac{\partial 1}{\partial x}.$$

Flux differencing: recovering split formulations

- Entropy conservative flux for Burgers' equation

$$f_S(u_L, u_R) = \frac{1}{6}\left(u_L^2 + u_L u_R + u_R^2\right).$$

- Flux differencing: let $u_L = u(x), u_R = u(y)$

$$\frac{\partial f(u)}{\partial x} \Longrightarrow 2\frac{\partial f_S\left(u(x), u(y)\right)}{\partial x}\Big|_{y=x}$$

- Recovering the Burgers' split formulation

$$f_S(u(x), u(y)) = \frac{1}{6}\left(u(x)^2 + u(x)u(y) + u(y)^2\right)$$

$$2\frac{\partial f_S\left(u(x), u(y)\right)}{\partial x}\Big|_{y=x} = \frac{1}{3}\frac{\partial u^2}{\partial x} + \frac{1}{3}u\frac{\partial u}{\partial x} + \frac{1}{3}u^2\cancel{\frac{\partial 1}{\partial x}}.$$

Flux differencing: beyond split formulations

- Fluxes do not necessarily correspond to split formulations!
- Example: entropy conservative flux for 1D compressible Euler

$$
\begin{aligned}
f_S^1(\boldsymbol{u}_L, \boldsymbol{u}_R) &= \{\{\rho\}\}^{\log} \{\{u\}\} \\
f_S^2(\boldsymbol{u}_L, \boldsymbol{u}_R) &= \frac{\{\{\rho\}\}}{2\{\{\beta\}\}} + \{\{u\}\} f_S^1 \\
f_S^3(\boldsymbol{u}_L, \boldsymbol{u}_R) &= f_S^1 \left(\frac{1}{2(\gamma-1)\{\{\beta\}\}^{\log}} - \frac{1}{2}\{\{u^2\}\} \right) + \{\{u\}\} f_S^2,
\end{aligned}
$$

- Logarithmic mean and "inverse temperature" β

$$
\{\{u\}\}^{\log} = \frac{u_L - u_R}{\log u_L - \log u_R}, \qquad \beta = \frac{\rho}{2p}.
$$

Chandreshekar (2013), *Kinetic energy preserving and entropy stable FV schemes for comp. Euler and NS equations.*

Flux differencing: implementational details

- Define $\boldsymbol{F}_S$ as evaluation of $\boldsymbol{f}_S$ at all combinations of quadrature points

$$(\boldsymbol{F}_S)_{ij} = (u(\boldsymbol{x}_i), u(\boldsymbol{x}_j)), \qquad \boldsymbol{x} = \left[\boldsymbol{x}^q, \boldsymbol{x}^f\right]^T.$$

- Replace $\frac{\partial}{\partial x}$ with $\boldsymbol{D}_N$ + projection and lifting matrices.

$$2\frac{\partial f_S\left(u(x), u(y)\right)}{\partial x}\bigg|_{y=x} \Longrightarrow \left[\begin{array}{cc} \boldsymbol{P}_q & \boldsymbol{L}_f \end{array}\right] \operatorname{diag}(2\boldsymbol{D}_N \boldsymbol{F}_S).$$

- Efficient Hadamard product reformulation of flux differencing (efficient on-the-fly evaluation of $\boldsymbol{F}_S$)

$$\operatorname{diag}(2\boldsymbol{D}_N \boldsymbol{F}_S) = (2\boldsymbol{D}_N \circ \boldsymbol{F}_S)\,\boldsymbol{1}.$$

Flux differencing: avoiding the chain rule

- Test with entropy variables $\widetilde{\boldsymbol{v}}$, integrate, and use SBP property:

$$\widetilde{\boldsymbol{v}}^T \left(2\boldsymbol{Q}_N \circ \boldsymbol{F}_S\right)\mathbf{1} = \widetilde{\boldsymbol{v}}^T \left(\left(\begin{bmatrix} 0 & \\ & \boldsymbol{W}_f \boldsymbol{n} \end{bmatrix} + \boldsymbol{Q}_N - \boldsymbol{Q}_N^T\right) \circ \boldsymbol{F}_S\right)\mathbf{1}.$$

- Only boundary terms appear in final estimate; volume terms become boundary terms using properties of $\left(\boldsymbol{F}_S\right)_{ij} = \boldsymbol{f}_S\left(\widetilde{\boldsymbol{u}}_i, \widetilde{\boldsymbol{u}}_j\right)$

$$\widetilde{\boldsymbol{v}}^T \left(\left(\boldsymbol{Q}_N - \boldsymbol{Q}_N^T\right) \circ \boldsymbol{F}_S\right)\mathbf{1} = \widetilde{\boldsymbol{v}}^T \left(\boldsymbol{Q}_N \circ \boldsymbol{F}_S\right)\mathbf{1} - \mathbf{1}^T \left(\boldsymbol{Q}_N \circ \boldsymbol{F}_S\right)\widetilde{\boldsymbol{v}}$$
$$= \sum_{i,j} \left(\boldsymbol{Q}_N\right)_{ij} \left(\widetilde{\boldsymbol{v}}_i - \widetilde{\boldsymbol{v}}_j\right)^T \boldsymbol{f}_S\left(\widetilde{\boldsymbol{u}}_i, \widetilde{\boldsymbol{u}}_j\right).$$

- Proof requires $\widetilde{\boldsymbol{v}} = \boldsymbol{v}(\widetilde{\boldsymbol{u}})$; the entropy variables $\widetilde{\boldsymbol{v}}$ must be a function of the conservative variables $\widetilde{\boldsymbol{u}}$.

Flux differencing: avoiding the chain rule

- Test with entropy variables $\widetilde{\boldsymbol{v}}$, integrate, and use SBP property:

$$\widetilde{\boldsymbol{v}}^T \left(2\boldsymbol{Q}_N \circ \boldsymbol{F}_S\right)\boldsymbol{1} = \widetilde{\boldsymbol{v}}^T \left(\left(\begin{bmatrix} 0 & \\ & \boldsymbol{W}_f \boldsymbol{n} \end{bmatrix} + \boldsymbol{Q}_N - \boldsymbol{Q}_N^T\right) \circ \boldsymbol{F}_S\right)\boldsymbol{1}.$$

- Only boundary terms appear in final estimate; volume terms become boundary terms using properties of $\left(\boldsymbol{F}_S\right)_{ij} = \boldsymbol{f}_S\left(\widetilde{\boldsymbol{u}}_i, \widetilde{\boldsymbol{u}}_j\right)$

$$\widetilde{\boldsymbol{v}}^T \left(\left(\boldsymbol{Q}_N - \boldsymbol{Q}_N^T\right) \circ \boldsymbol{F}_S\right)\boldsymbol{1} = \widetilde{\boldsymbol{v}}^T \left(\boldsymbol{Q}_N \circ \boldsymbol{F}_S\right)\boldsymbol{1} - \boldsymbol{1}^T \left(\boldsymbol{Q}_N \circ \boldsymbol{F}_S\right)\widetilde{\boldsymbol{v}}$$
$$= \sum_{i,j} \left(\boldsymbol{Q}_N\right)_{ij} \left(\psi(\widetilde{\boldsymbol{u}}_i) - \psi(\widetilde{\boldsymbol{u}}_j)\right).$$

- Proof requires $\widetilde{\boldsymbol{v}} = \boldsymbol{v}(\widetilde{\boldsymbol{u}})$; the entropy variables $\widetilde{\boldsymbol{v}}$ must be a function of the conservative variables $\widetilde{\boldsymbol{u}}$.

Flux differencing: avoiding the chain rule

- Test with entropy variables $\widetilde{\boldsymbol{v}}$, integrate, and use SBP property:

$$\widetilde{\boldsymbol{v}}^T \left(2\boldsymbol{Q}_N \circ \boldsymbol{F}_S\right)\mathbf{1} = \widetilde{\boldsymbol{v}}^T \left(\left(\begin{bmatrix} 0 & \\ & \boldsymbol{W}_f \boldsymbol{n} \end{bmatrix} + \boldsymbol{Q}_N - \boldsymbol{Q}_N^T\right) \circ \boldsymbol{F}_S\right)\mathbf{1}.$$

- Only boundary terms appear in final estimate; volume terms become boundary terms using properties of $\left(\boldsymbol{F}_S\right)_{ij} = \boldsymbol{f}_S\left(\widetilde{\boldsymbol{u}}_i, \widetilde{\boldsymbol{u}}_j\right)$

$$\begin{aligned}\widetilde{\boldsymbol{v}}^T \left(\left(\boldsymbol{Q}_N - \boldsymbol{Q}_N^T\right) \circ \boldsymbol{F}_S\right)\mathbf{1} &= \widetilde{\boldsymbol{v}}^T \left(\boldsymbol{Q}_N \circ \boldsymbol{F}_S\right)\mathbf{1} - \mathbf{1}^T \left(\boldsymbol{Q}_N \circ \boldsymbol{F}_S\right)\widetilde{\boldsymbol{v}} \\ &= \mathbf{1}^T \boldsymbol{Q}_N \psi - \psi^T \boldsymbol{Q}_N \mathbf{1} = \mathbf{1}^T \boldsymbol{Q}_N \psi\end{aligned}$$

- Proof requires $\widetilde{\boldsymbol{v}} = \boldsymbol{v}(\widetilde{\boldsymbol{u}})$; the entropy variables $\widetilde{\boldsymbol{v}}$ must be a function of the conservative variables $\widetilde{\boldsymbol{u}}$.

Flux differencing: avoiding the chain rule

- Test with entropy variables $\widetilde{\boldsymbol{v}}$, integrate, and use SBP property:

$$\widetilde{\boldsymbol{v}}^T \left(2\boldsymbol{Q}_N \circ \boldsymbol{F}_S\right)\mathbf{1} = \widetilde{\boldsymbol{v}}^T \left(\left(\begin{bmatrix} 0 & \\ & \boldsymbol{W}_f \boldsymbol{n} \end{bmatrix} + \boldsymbol{Q}_N - \boldsymbol{Q}_N^T\right) \circ \boldsymbol{F}_S\right)\mathbf{1}.$$

- Only boundary terms appear in final estimate; volume terms become boundary terms using properties of $\left(\boldsymbol{F}_S\right)_{ij} = \boldsymbol{f}_S\left(\widetilde{\boldsymbol{u}}_i, \widetilde{\boldsymbol{u}}_j\right)$

$$\widetilde{\boldsymbol{v}}^T \left(\left(\boldsymbol{Q}_N - \boldsymbol{Q}_N^T\right) \circ \boldsymbol{F}_S\right)\mathbf{1} = \widetilde{\boldsymbol{v}}^T \left(\boldsymbol{Q}_N \circ \boldsymbol{F}_S\right)\mathbf{1} - \mathbf{1}^T \left(\boldsymbol{Q}_N \circ \boldsymbol{F}_S\right)\widetilde{\boldsymbol{v}}$$
$$= \mathbf{1}^T \left(\boldsymbol{B}_N - \boldsymbol{Q}_N^T\right)\psi = \mathbf{1}^T \boldsymbol{B}_N \psi.$$

- Proof requires $\widetilde{\boldsymbol{v}} = \boldsymbol{v}(\widetilde{\boldsymbol{u}})$; the entropy variables $\widetilde{\boldsymbol{v}}$ must be a function of the conservative variables $\widetilde{\boldsymbol{u}}$.

Flux differencing: avoiding the chain rule

- Test with entropy variables $\widetilde{\boldsymbol{v}}$, integrate, and use SBP property:

$$\widetilde{\boldsymbol{v}}^T \left(2\boldsymbol{Q}_N \circ \boldsymbol{F}_S\right)\boldsymbol{1} = \widetilde{\boldsymbol{v}}^T \left(\left(\begin{bmatrix} 0 & \\ & \boldsymbol{W}_f \boldsymbol{n} \end{bmatrix} + \boldsymbol{Q}_N - \boldsymbol{Q}_N^T\right) \circ \boldsymbol{F}_S\right)\boldsymbol{1}.$$

- Only boundary terms appear in final estimate; volume terms become boundary terms using properties of $\left(\boldsymbol{F}_S\right)_{ij} = \boldsymbol{f}_S\left(\widetilde{\boldsymbol{u}}_i, \widetilde{\boldsymbol{u}}_j\right)$

$$\widetilde{\boldsymbol{v}}^T \left(\left(\boldsymbol{Q}_N - \boldsymbol{Q}_N^T\right) \circ \boldsymbol{F}_S\right)\boldsymbol{1} = \widetilde{\boldsymbol{v}}^T \left(\boldsymbol{Q}_N \circ \boldsymbol{F}_S\right)\boldsymbol{1} - \boldsymbol{1}^T \left(\boldsymbol{Q}_N \circ \boldsymbol{F}_S\right)\widetilde{\boldsymbol{v}}$$
$$= \boldsymbol{1}^T \left(\boldsymbol{B}_N - \boldsymbol{Q}_N^T\right)\psi = \boldsymbol{1}^T \boldsymbol{B}_N \psi.$$

- Proof requires $\widetilde{\boldsymbol{v}} = \boldsymbol{v}(\widetilde{\boldsymbol{u}})$; the entropy variables $\widetilde{\boldsymbol{v}}$ must be a function of the conservative variables $\widetilde{\boldsymbol{u}}$.

Modifying the conservative variables

- Conservative variables $\boldsymbol{u}_h$ and test functions are polynomial, but the entropy variables $\boldsymbol{v}(\boldsymbol{u}_h) \notin P^N$!
- Evaluate flux $\boldsymbol{f}_S$ using modified conservative variables $\widetilde{\boldsymbol{u}}$

$$\widetilde{\boldsymbol{u}} = \boldsymbol{u}\left(P_N \boldsymbol{v}(\boldsymbol{u}_h)\right).$$

- If $\boldsymbol{v}(\boldsymbol{u})$ is an invertible mapping, this choice of $\widetilde{\boldsymbol{u}}$ ensures that

$$\widetilde{\boldsymbol{v}} = \boldsymbol{v}(\widetilde{\boldsymbol{u}}) = P_N \boldsymbol{v}(\boldsymbol{u}_h) \in P^N.$$

- Local conservation w.r.t. a generalized Lax-Wendroff theorem.

Shi and Shu (2017). *On local conservation of numerical methods for conservation laws.*

A discretely entropy conservative DG method

Theorem (Chan 2018)

Let $\boldsymbol{u}_h(\boldsymbol{x}) = \sum_j \widehat{\boldsymbol{u}}_j \phi_j(\boldsymbol{x})$ *and* $\widetilde{\boldsymbol{u}} = \boldsymbol{u}\left(P_N \boldsymbol{v}\right)$*. Let* $\widehat{\boldsymbol{u}}$ *locally solve*

$$\frac{\mathrm{d}\widehat{\boldsymbol{u}}}{\mathrm{d}t} + \sum_{i=1}^{d} \begin{bmatrix} \boldsymbol{P}_q & \boldsymbol{L}_f \end{bmatrix} \left(2\boldsymbol{D}_N^i \circ \boldsymbol{F}_S^i\right)\mathbf{1} + \boldsymbol{L}_f \left(\boldsymbol{f}_S^i(\widetilde{\boldsymbol{u}}^+, \widetilde{\boldsymbol{u}}) - \boldsymbol{f}^i(\widetilde{\boldsymbol{u}})\right)\boldsymbol{n}_i = 0.$$

Assuming continuity in time, $\boldsymbol{u}_h(\boldsymbol{x})$ *satisfies the quadrature form of*

$$\int_\Omega \frac{\partial S(\boldsymbol{u}_h)}{\partial t} + \sum_{i=1}^{d} \int_{\partial\Omega} \left(\left(P_N \boldsymbol{v}\right)^T \boldsymbol{f}^i(\widetilde{\boldsymbol{u}}) - \psi_i(\widetilde{\boldsymbol{u}})\right)\boldsymbol{n}_i = 0.$$

- Can modify interface flux (e.g. Lax-Friedrichs or matrix dissipation) to change the entropy equality to an entropy inequality.

Winters, Derigs, Gassner, and Walch (2017). *A uniquely defined entropy stable matrix dissipation operator for high Mach number ideal MHD and compressible Euler simulations.*

Talk outline

1 Stability of DG: linear PDEs vs nonlinear conservation laws

2 Summation by parts finite differences

3 High order DG and summation by parts

4 Entropy stable formulations and flux differencing

5 Numerical experiments
- Triangular and tetrahedral meshes
- Quadrilateral and hexahedral meshes

1D compressible Euler equations

- Inexact Gauss-Legendre-Lobatto (GLL) vs Gauss (GQ) quadratures.
- Entropy conservative (EC) and Lax-Friedrichs (LF) fluxes.
- No additional stabilization, filtering, or limiting.

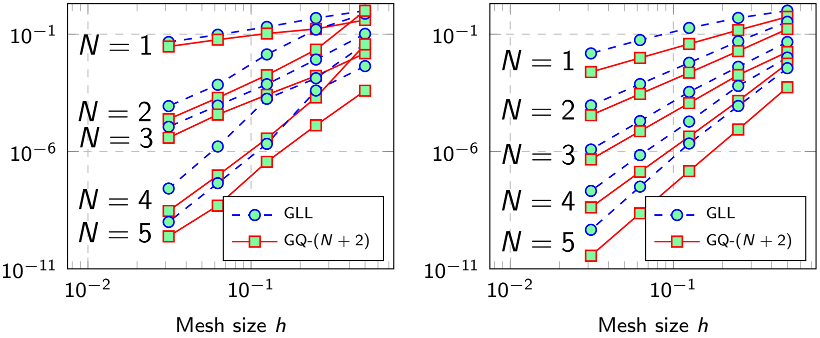

(a) Entropy conservative flux

(b) With Lax-Friedrichs penalization

Conservation of entropy: fully discrete schemes

- Entropy conservation: *semi-discrete*, not fully discrete.
- $\Delta S(\boldsymbol{u}) = |S(\boldsymbol{u}(x,t)) - S(\boldsymbol{u}(x,0))| \to 0$ as as $\Delta t \to 0$.

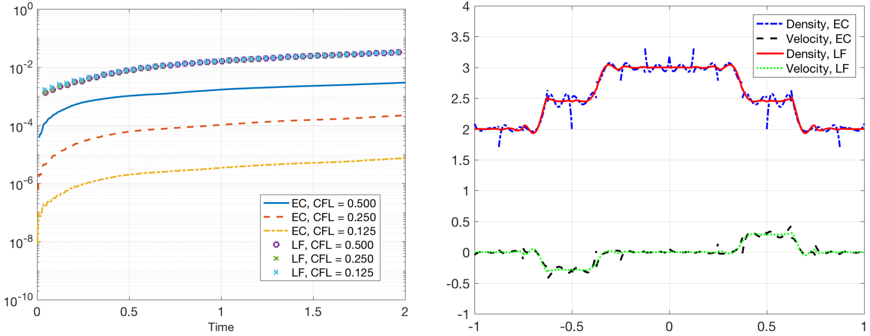

(a) $\Delta S(\boldsymbol{u})$ for various Δt (b) $\rho(x), u(x)$ ($N = 4, K = 16$)

Solution and change in entropy $\Delta S(\boldsymbol{u})$ for entropy conservative (EC) and Lax-Friedrichs (LF) fluxes (using GQ-$(N+2)$ quadrature).

1D Sod shock tube

- Circles are cell averages.
- CFL of .125 used for both GLL-$(N+1)$and GQ-$(N+2)$.

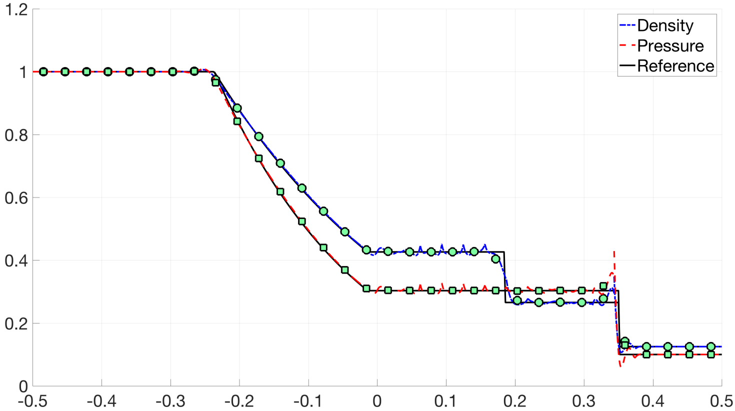

$N = 4$, $K = 32$, $(N + 1)$ point Gauss-Lobatto-Legendre quadrature.

1D Sod shock tube

- Circles are cell averages.
- CFL of .125 used for both GLL-$(N+1)$and GQ-$(N+2)$.

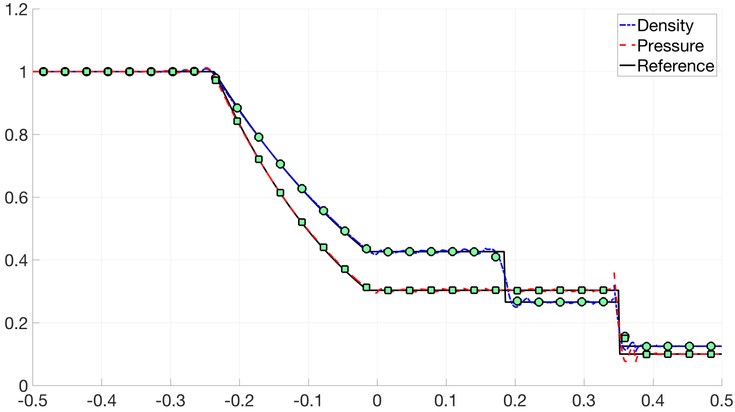

$N = 4$, $K = 32$, $(N+2)$ point Gauss quadrature.

1D sine-shock interaction

- GQ-$(N+2)$ needs smaller CFL (.05 vs .125) for stability.

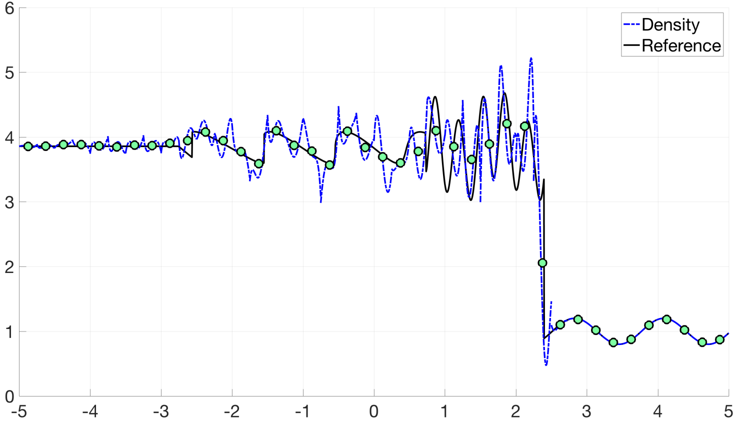

$N = 4$, $K = 40$, $CFL = .05$, $(N+1)$ point Gauss-Lobatto-Legendre quadrature.

1D sine-shock interaction

- GQ-$(N+2)$ needs smaller CFL (.05 vs .125) for stability.

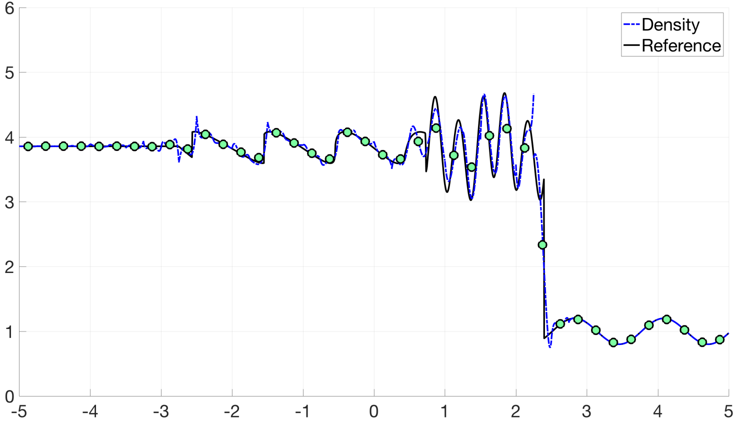

$N = 4$, $K = 40$, $CFL = .05$, $(N+2)$ point Gauss quadrature.

Talk outline

1 Stability of DG: linear PDEs vs nonlinear conservation laws

2 Summation by parts finite differences

3 High order DG and summation by parts

4 Entropy stable formulations and flux differencing

5 Numerical experiments
- Triangular and tetrahedral meshes
- Quadrilateral and hexahedral meshes

2D Riemann problem

- Uniform 64×64 mesh: $N = 3$, CFL .125, Lax-Friedrichs stabilization.
- No limiting or artificial viscosity required to maintain stability!
- Periodic on larger domain ("natural" boundary conditions unstable).

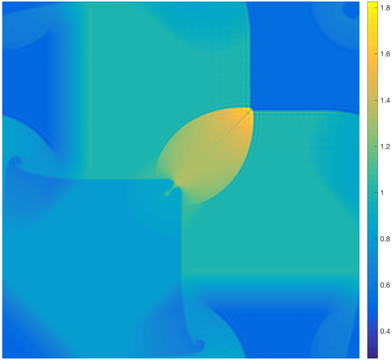

(a) $\Omega = [-1, 1]^2$

(b) $\Omega = [-.5, .5]^2$, 32×32 elements

Smooth isentropic vortex and curved meshes in 2D/3D

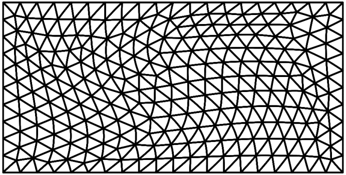

(a) 2D triangular mesh

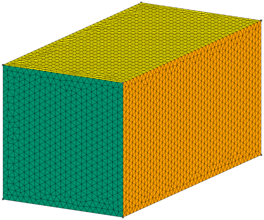

(b) 3D tetrahedral mesh

Figure: Example of 2D and 3D meshes used for convergence experiments.

- Entropy stability: needs discrete geometric conservation law (GCL).
- Generalized mass lumping for curved: weight-adjusted mass matrices.
- Modify $\widetilde{\boldsymbol{u}} = \boldsymbol{u}\left(\widetilde{\boldsymbol{v}}\right)$, $\widetilde{\boldsymbol{v}} = \widetilde{P}_N^k \boldsymbol{v}(\boldsymbol{u}_h)$ using weight-adjusted projection $\widetilde{P}_N^k$.

Visbal and Gaitonde (2002). On the Use of Higher-Order Finite-Difference Schemes on Curvilinear and Deforming Meshes.
Kopriva (2006). Metric identities and the discontinuous spectral element method on curvilinear meshes.
Chan, Hewett, and Warburton (2016). *Weight-adjusted discontinuous Galerkin methods: curvilinear meshes.*

Smooth isentropic vortex and curved meshes in 2D/3D

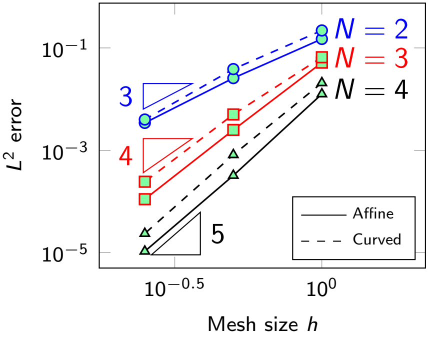

(a) 2D results

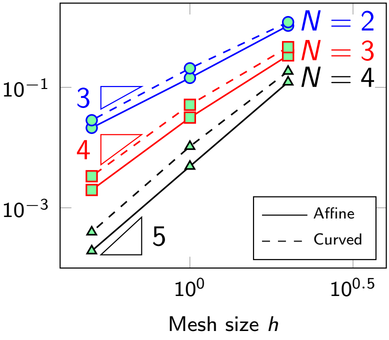

(b) 3D results

L^2 errors for 2D/3D isentropic vortex at $T = 5$ on affine, curved meshes.

Visbal and Gaitonde (2002). On the Use of Higher-Order Finite-Difference Schemes on Curvilinear and Deforming Meshes.
Kopriva (2006). Metric identities and the discontinuous spectral element method on curvilinear meshes.
Chan, Hewett, and Warburton (2016). *Weight-adjusted discontinuous Galerkin methods: curvilinear meshes.*

Taylor-Green vortex

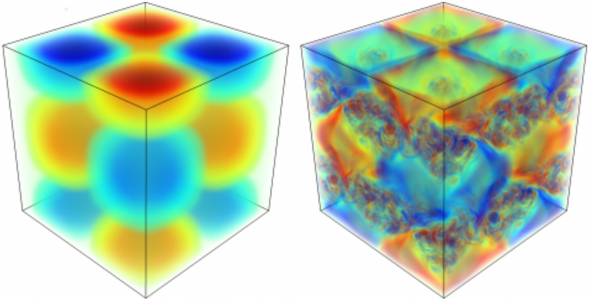

Figure: Isocontours of z-vorticity for Taylor-Green at $t = 0, 10$ seconds.

- Simple turbulence-like behavior (generation of small scales).
- Inviscid Taylor-Green: tests robustness w.r.t. under-resolved solutions.

https://how4.cenaero.be/content/bs1-dns-taylor-green-vortex-re1600.

Taylor-Green vortex: kinetic energy dissipation rate

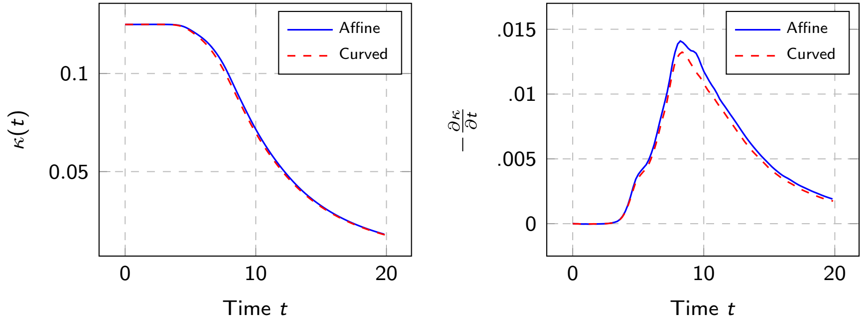

(a) Kinetic energy (b) KE dissipation rate

Figure: Evolution of kinetic energy $\kappa(t)$ and kinetic energy dissipation rate $-\frac{\partial \kappa}{\partial t}$ for $N = 3, h = \pi/8, \mathrm{CFL} = .25$ on affine and curved meshes of $[-\pi, \pi]^3$.

Gassner, Winters, Kopriva (2016). *Split form nodal DG schemes with SBP property for the compressible Euler equations.*

Taylor-Green vortex: kinetic energy dissipation rate

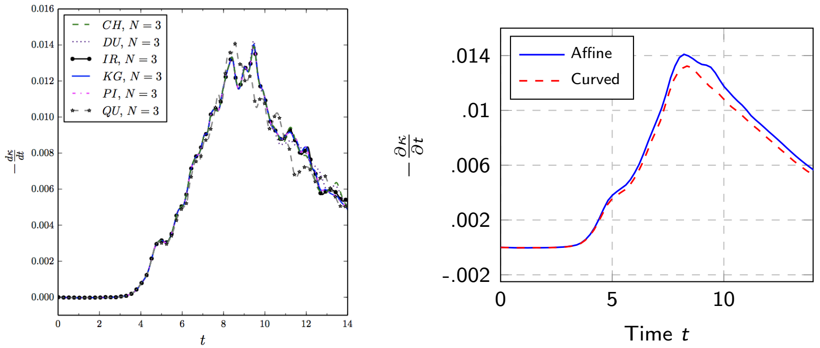

(a) KE dissipation rate from Gassner, Winters, Kopriva (2016)

(b) KE dissipation rate

Figure: Evolution of kinetic energy $\kappa(t)$ and kinetic energy dissipation rate $-\frac{\partial \kappa}{\partial t}$ for $N = 3, h = \pi/8, \mathrm{CFL} = .25$ on affine and curved meshes of $[-\pi, \pi]^3$.

Gassner, Winters, Kopriva (2016). *Split form nodal DG schemes with SBP property for the compressible Euler equations.*

Talk outline

1 Stability of DG: linear PDEs vs nonlinear conservation laws

2 Summation by parts finite differences

3 High order DG and summation by parts

4 Entropy stable formulations and flux differencing

5 Numerical experiments
- Triangular and tetrahedral meshes
- Quadrilateral and hexahedral meshes

Entropy stable Gauss collocation: main steps

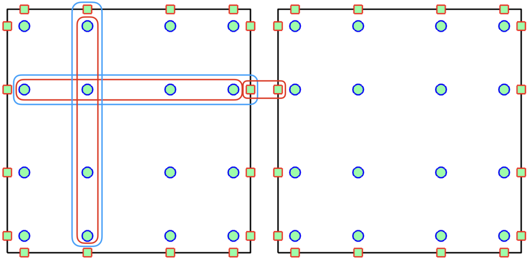

- Advantage over tetrahedral elements: tensor product structure.
- Reduces computational costs from $O(N^6)$ to $O(N^4)$ in 3D.
- New approach: collocation at Gauss nodes instead of GLL nodes.

Improved errors on curved meshes

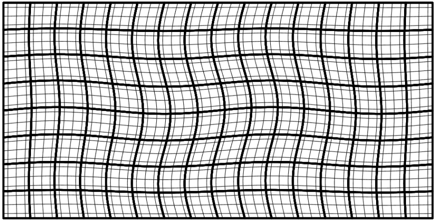

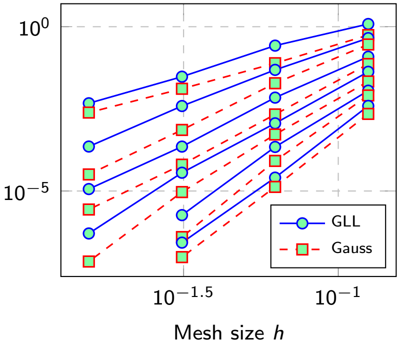

Figure: L^2 errors for the 2D isentropic vortex at time $T = 5$ for degree $N = 2, \ldots, 7$ GLL and Gauss collocation schemes (similar behavior in 3D).

Improved errors on curved meshes

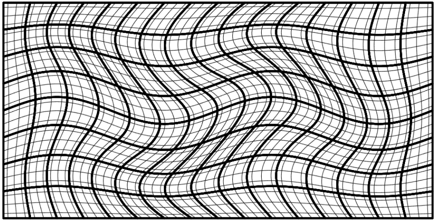

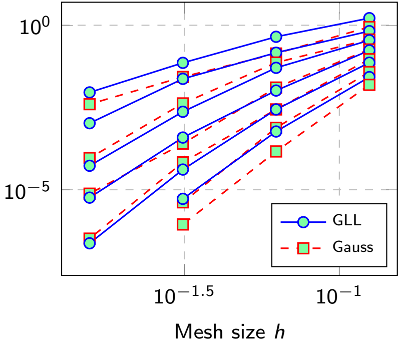

Figure: L^2 errors for the 2D isentropic vortex at time $T = 5$ for degree $N = 2, \ldots, 7$ GLL and Gauss collocation schemes (similar behavior in 3D).

Improved errors on curved meshes

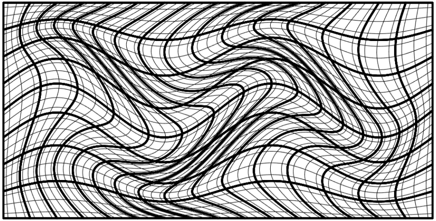

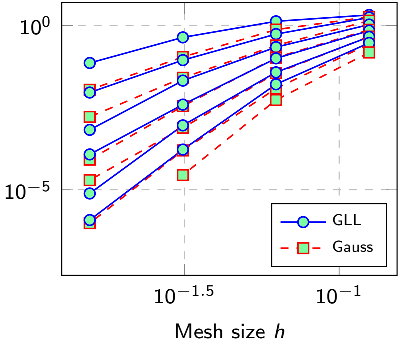

Figure: L^2 errors for the 2D isentropic vortex at time $T = 5$ for degree $N = 2, \ldots, 7$ GLL and Gauss collocation schemes (similar behavior in 3D).

Shock vortex interaction

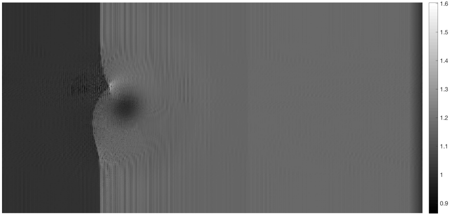

(a) Entropy conservative flux, $T = .3$

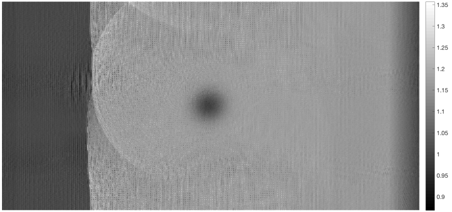

(b) Entropy conservative flux, $T = .7$

Figure: Shock vortex interaction problem using high order entropy stable Gauss collocation schemes with $N = 4, h = 1/100$.

Winters, Derigs, Gassner, and Walch (2017). *A uniquely defined entropy stable matrix dissipation operator for high Mach number ideal MHD and compressible Euler simulations.*

Shock vortex interaction

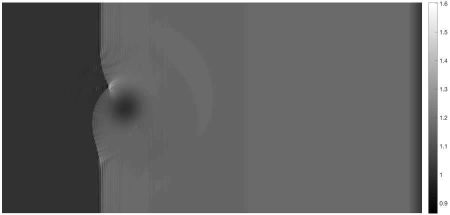

(a) Lax-Friedrichs flux, $T = .3$

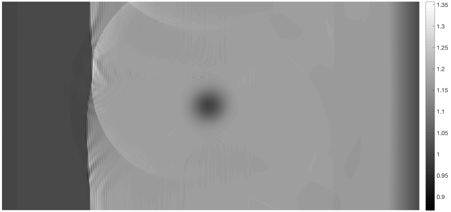

(b) Lax-Friedrichs flux, $T = .7$

Figure: Shock vortex interaction problem using high order entropy stable Gauss collocation schemes with $N = 4, h = 1/100$.

Winters, Derigs, Gassner, and Walch (2017). *A uniquely defined entropy stable matrix dissipation operator for high Mach number ideal MHD and compressible Euler simulations.*

Shock vortex interaction

(a) Matrix dissipation flux, $T = .3$

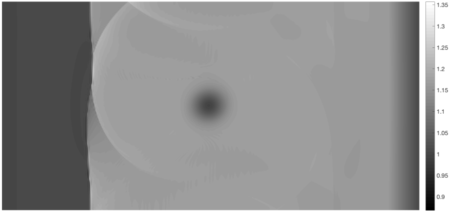

(b) Matrix dissipation flux, $T = .7$

Figure: Shock vortex interaction problem using high order entropy stable Gauss collocation schemes with $N = 4, h = 1/100$.

Winters, Derigs, Gassner, and Walch (2017). *A uniquely defined entropy stable matrix dissipation operator for high Mach number ideal MHD and compressible Euler simulations.*

Shock vortex interaction

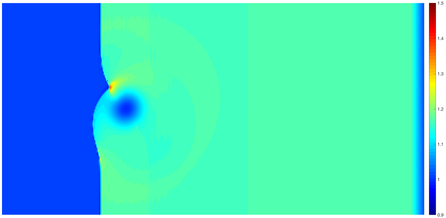

(a) Matrix dissipation flux, $T = .3$

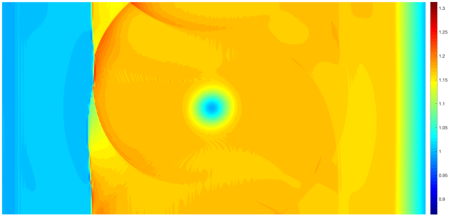

(b) Matrix dissipation flux, $T = .7$

Figure: Shock vortex interaction problem using high order entropy stable Gauss collocation schemes with $N = 4, h = 1/100$.

Winters, Derigs, Gassner, and Walch (2017). *A uniquely defined entropy stable matrix dissipation operator for high Mach number ideal MHD and compressible Euler simulations.*

Summary and future work

- Discretely stable time-domain high order discontinuous Galerkin methods: provable semi-discrete stability, excellent GPU efficiency.[1]
- Additional work required: strong shocks, positivity preservation.
- Currently: hybrid meshes, continuous FEM, regularization (limiting, artificial viscosity), multi-GPU (with Lucas Wilcox).
- This work is supported by DMS-1719818.

Thank you! Questions?

Chan, Del Rey Fernandez, Carpenter (2018). *Efficient entropy stable Gauss collocation methods*.

Chan, Wilcox (2018). *On discretely entropy stable weight-adjusted DG methods: curvilinear meshes*.

Chan (2017). *On discretely entropy conservative and entropy stable discontinuous Galerkin methods*.

Additional slides

Over-integration is ineffective without L^2 projection

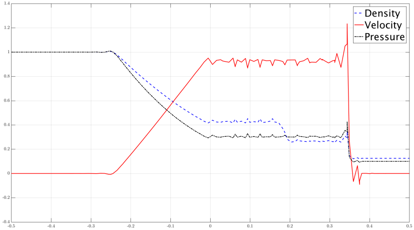

(a) $(N+1)$ points

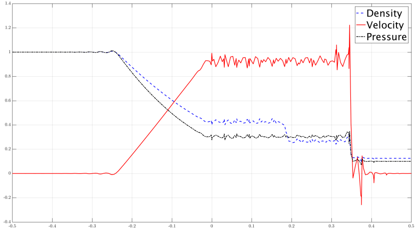

(b) $(N+4)$ points

Figure: Numerical results for the Sod shock tube for $N = 4$ and $K = 32$ elements. Over-integrating by increasing the number of quadrature points does not improve solution quality.

On CFL restrictions

- For GLL-$(N+1)$ quadrature, $\widetilde{\boldsymbol{u}} = \boldsymbol{u}\left(P_N \boldsymbol{v}\right) = \boldsymbol{u}$ at GLL points.
- For GQ-$(N+2)$, discrepancy between L^2 projection and interpolation.
- Still need positivity of thermodynamic quantities for stability!

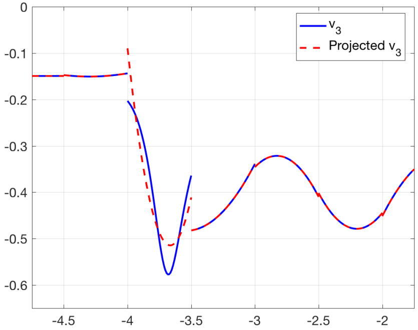

(a) $v_3(x), \left(P_N v_3\right)(x)$

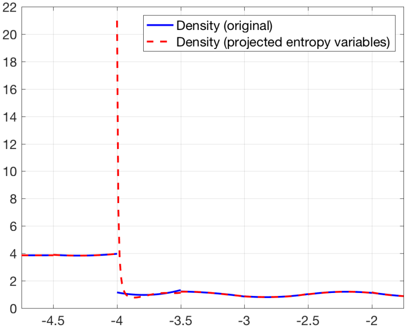

(b) $\rho(x), \rho\left(\left(P_N \boldsymbol{v}\right)(x)\right)$

High order DG on many-core (GPU) architectures

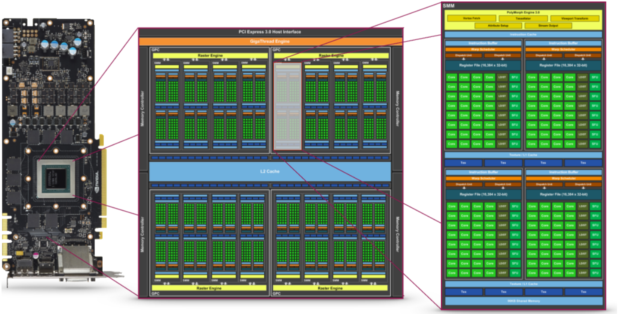

Figure: NVIDIA Maxwell GM204 GPU: 16 cores, 4 SIMD clusters of 32 units.

- Thousands of processing units organized in synchronized groups.
- No free lunch: memory costs (accesses, transfer, latency, storage).

Klockner, Warburton, Bridge, Hesthaven 2009, Nodal discontinuous Galerkin methods on graphics processors.

High order DG on many-core (GPU) architectures

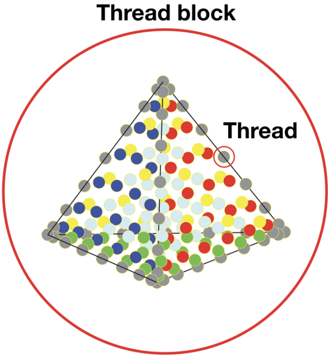

Figure: Thread blocks process elements, threads process degrees of freedom.

- Thousands of processing units organized in synchronized groups.
- No free lunch: memory costs (accesses, transfer, latency, storage).

Klockner, Warburton, Bridge, Hesthaven 2009, Nodal discontinuous Galerkin methods on graphics processors.

High order DG on many-core (GPU) architectures

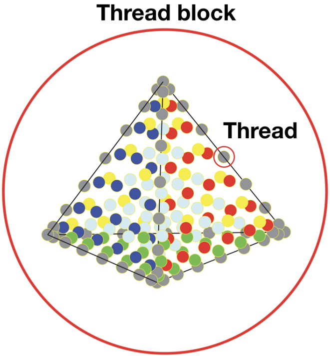

Figure: Thread blocks process elements, threads process degrees of freedom.

- Thousands of processing units organized in synchronized groups.
- No free lunch: memory costs (accesses, transfer, latency, storage).

Klockner, Warburton, Bridge, Hesthaven 2009, Nodal discontinuous Galerkin methods on graphics processors.

Implementing high order entropy stable DG on GPUs

- "FLOPS are free, **but** ..."

  (bytes are expensive) / (memory is dear) / (postage is extra)

- Standard considerations: minimize CPU-GPU transfers, structured data layouts, reduce global memory accesses, maximize data reuse.

- Arithmetic vs memory latency: need roughly $O(10)$ operations per byte of memory accessed (high arithmetic intensity).

- Standard mat-vec: only $1/10 - 1/2$ FLOPS per byte!

GPUs and flux differencing: when FLOPS are free

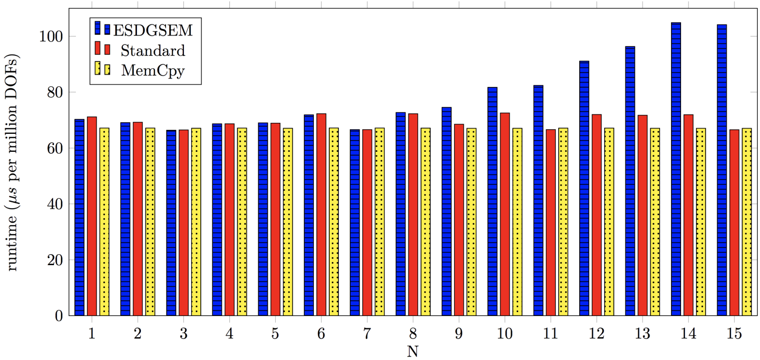

- High arithmetic intensity: compute while waiting for global memory.
- On GPUs, extra operations don't increase runtime until $N \geq 9$!

Wintermeyer, Winters, Gassner, Warburton (2018). *An entropy stable discontinuous Galerkin method for the shallow water equations on curvilinear meshes with wet/dry fronts accelerated by GPUs.*